INVESTIGATIONS ON STACKED APERTURE COUPLED FRACTAL MICROSTRIP ANTENNAS FOR WIRELESS COMMUNICATION APPLICATIONS

A Thesis Submitted in Partial Fulfillment of the Requirement for the Award of the Degree of

MASTER OF ENGINEERING
IN
WIRELESS COMMUNICATION

Submitted by

KUMARI LAXMI

Roll No. 801663003

Under Supervision of

Dr. Amanpreet Kaur
Assistant Professor, ECED, TIET
&
Dr. Amit Kumar Kohli
Associate Professor, ECED, TIET

THAPAR INSTITUTE
OF ENGINEERING & TECHNOLOGY
(Deemed to be University)

ELECTRONICS AND COMMUNICATION ENGINEERING DEPARTMENT
THAPAR INSTITUTE OF ENGINEERING & TECHNOLOGY
(A DEEMED TO BE UNIVERSITY), PATIALA, PUNJAB, INDIA
JULY, 2018

DECLARATION

I, Kumari Laxmi, hereby declare that the work presented in this thesis entitled **"Investigations on Stacked Aperture Coupled Fractal Microstrip Antennas for Wireless Communication Applications,"** in the partial fulfillment of the requirement for the award of degree of Master of Engineering (Wireless Communication) submitted in Electronics and Communication Engineering Department, Thapar Institute of Engineering & Technology (T.I.E.T., Deemed University), Patiala, India is an authentic record of my own work carried out under the supervision/guidance of **Dr. Amanpreet Kaur** (Assistant Professor) and **Dr. Amit Kumar Kohli** (Associate Professor), Electronics and Communication Engineering Department, T.I.E.T., Patiala from July 2017 to July 2018.

The matter presented in this thesis has not been submitted either in part or full to any other university or institute for the award of any other degree.

Date: 5th July 2018

Kumari Laxmi
Roll No: 801663003

It is certified that the above statement made by the candidate is correct to the best of my knowledge and belief.

Date: 5.7.18.

Dr. Amanpreet Kaur 5/7/18
Assistant Professor, ECED
T.I.E.T., Patiala, Punjab, India

Date: 6/7/2018

Dr. Amit Kumar Kohli 6/7/2018
Associate Professor, ECED
T.I.E.T., Patiala, Punjab, India

ACKNOWLEDGEMENT

First of all, I express my sincere thanks to the all almighty GOD for honoring me with knowledge, intelligence, well-being, cognizance and the brainpower to conduct this research successfully.

I wish to express my deep gratitude and sincere thanks to my supervisors, **Dr. Amanpreet Kaur** (Assistant Professor), and **Dr. Amit Kumar Kohli** (Associate Professor), Electronics and Communication Engineering Department (ECED), T.I.E.T., Patiala, for their invaluable guidance, constant encouragement, constructive comments, sympathetic attitude, and immense motivation, which has sustained my efforts at all stages of this work. Their valuable advice and suggestions for the corrections, modifications and improvement did enhance my work.

I would like to express my gratitude to **Dr. Alpana Agarwal**, The Head of Electronics and Communication Department (ECED), T.I.E.T., Patiala, for providing me with adequate environment in carrying out the work. I am also thankful to the PG coordinator, **Dr. A.K. Singh**, Electronics and Communication Engineering Department (ECED).

Finally, I want to extend my gratitude to all those persons who directly or indirectly helped me in carrying out this work in right direction.

Kumari Laxmi
(801663003)

ABSTRACT

The wireless industry has undergone an advanced technical revolution in present era. Antenna, the most important component in the wireless systems requires versatility and efficiency in order to support the demands of current wireless communication scenario. Apart from the demand for small-size antennas, the advanced wireless communication systems prefer multiband antennas, so as to cover maximum applications with a single antenna. Fractal microstrip antennas (MSAs) play the principle part by fulfilling such wireless signalling requirements. Fractal MSAs exhibit non-integral dimensional configurations, and their space-filling capabilities can be utilised for miniaturizing antenna size, and their characteristics of self-similarity in geometry result in the antennas having more number of resonant frequencies. Usually, fractal antennas doesn't need any matching components to attain multiband as well as broadband performances. Thus, the research work presented here in this thesis focuses on the design, simulation as well as testing of a stacked Sierpinski bow-tie antenna, and diamond shaped Sierpinski gasket fractal antenna.

The research work starts with the review on fractal antennas, and then Sierpinski gasket bow-tie antenna is designed using CST (Computer Simulation Software) microwave studio version 2017. This design is extended to a stacked structure (one layer of stacking) with three types of geometry namely: "driven and parasitic patches of same size", "parasitic patch smaller than driven patch", and "parasitic patch greater than the size of the given patch." The antennas are fed by utilising aperture coupled feeding mechanism because it provides reasonably higher bandwidth as compared to other feeds, and generates a moderate amount of spurious radiations. Stacked Sierpinski gasket fractal antenna with same active and parasitic patch covers the highest impedance bandwidth as compared to the other two geometries, and is therefore preferred. The obtained results are implemented on another design of stacked diamond Sierpinski gasket fractal antenna with similar dimensions of patches, which covers multiple resonant bands from 4.95 GHz to 5.04 GHz (90 MHz), 5.40 GHz to 6.72 GHz (1.32 GHz) and 6.95 GHz to 7.25 GHz (300 MHz). In order to validate the antenna application in practical wireless scenario, the two stacked structures with similar dimensions of driven and parasitic patch are fabricated by utilising photolithography process, and then tested on a VNA model no. E5063A. The measured results are quite matching with simulated ones allowing the antenna to be suitable for WLAN, UWB, G-band, E-band, radio communication, satellite communication, and radar communication applications.

Keywords: Fractal microstrip antenna, Sierpinski gasket, Bow-tie fractal antenna.

TABLE OF CONTENTS

LIST OF FIGURES

LIST OF TABLES

LIST OF ABBREVIATIONS

BW	*Bandwidth*
CSRR	*Complimentary Split Ring Resonator*
CST MWS	*Computers Simulation Tool Microwave Studio*
CPW	*Coplanar Waveguide*
DGS	*Defected Ground Structure*
EM	*Electromagnetic*
FR4	*Forgotten Realms 4*
GPS	*Global Positioning Systems*
IR	*Infrared*
ITU	*International Telecommunication Union*
LED	*Light Emitting Diode*
LOS	*Line of Sight*
MPA	*Microstrip Patch Antenna*
TEM	*Transfer Electric Mode*
TV	*Television*
U-NII	*Unsliced National Information Infrastructure*
UWB	*Ultra-Wide Band*
VHF/UHF	*Very High Frequency/ Ultra High Frequency*
VNA	*Vector Network Analyzer*
VSWR	*Voltage Standing Wave Ration*
Wi-Fi	*Wireless Fidelity*
WiMAX	*World Wide Interoperability for Microwave Access*
WLAN	*Wireless Local Area Network*

CHAPTER-1

INTRODUCTION

1.1 WIRELESS COMMUNICATION:

Among all the available technologies, wireless communication is a major contribution to the modern civilization. Without the use of cables, wires or any additional type of electrical conducting material, information can be communicated over a long distance by utilising wireless equipment. The distance of transmission is anywhere between a few meters (e.g., a T.V. remote control) and thousands of kilometres (e.g., radio transmission). Wireless transmission has become an essential part of human lives, as this permits mobile subscribers to transmit information even from remotely operated regions.

Wireless communication devices utilised for communication are mobiles, cordless telephones, GPS units, wireless computing equipments, as well as satellite T.V. The next section presents the types of wireless communication available to the users.

1.1.1 Types of Wireless Communication:

1.1.1.1 Satellite Communication:

Satellite communication is a self-contained wireless transmission technique, which is extensively spread all over globe to permit subscribes/customers to stay inter-connected almost everywhere in this world. When a signalling waveform (a beam of modulated microwave) is transmitted to the satellite, then the satellite amplifies this received signalling waveform, and transmits it back towards receiving antenna, that is situated at the particular place on earth. Satellite communication mainly encompasses two components, which are space-segment and ground-segment. Here, ground- segment is usually consisting of fixed/mobile transmitting, receiving as well as ancillary equipments; and however the space-segment is containing satellite itself. The distance covered in one hop of satellite communication is around 4000km [1].

1.1.1.2 Infrared Communication:

Infrared wireless communication equipment transmits information data through any device or by using infrared radiation systems. The infrared electromagnetic energy is at a wavelength higher

than the wavelength of red light. This is utilised for T.V. remote control, security controller as well as for short range communication. Microwaves and visible light are the two radiations near IR radiation spectrum, in the electromagnetic spectrum. Therefore, these may be utilised as a source to communicate between to end users. To achieve the successful infrared signal transmission, a photo light emitting diode based transmitting equipment and a photo diode based receiving equipment are needed. This is employed for short range indoor communication.

1.1.1.3 Broadcast Radio:

First wireless communication technique is an open radio transmission to seek out widespread usage, which is still serving this motive nowadays. Handy multichannel radios allow any subscriber to speak over small distances, whereas citizen's band as well as maritime radios offer signal transmission services for sailors. Ham radio enthusiasts share information signals and function emergency transmission/reception aids throughout disasters by utilizing some powerful broadcasting gear, and these may even transmit digital data signals over radio frequency spectrum. Radio signals are electromagnetic signalling waveforms, which are communicated by utilizing an antenna. Such signalling waveforms exhibit entirely different frequency segments, in which a user/subscriber can get excess of an audio signal just by varying the frequency segment.

1.1.1.4 Microwave Communication:

Microwave wireless communication is an effectual kind of transmission, which utilises radio waves, where wavelengths of radio waves are appearing to be in centimetres. Under this transmission scenario, information signals may be transferred by utilising two schemes. Here, first is satellite technology and other is terrestrial technology. However in satellite technology, information may be communicated via a concerned satellite, which orbits at about 22,300 miles above our planet. Station on earth sends as well as receives information signals from concerned satellite with a frequency ranging from 11 GHz -14 GHz, and at a transmission rate of 1 Mb/s to 10Mb/s. In terrestrial technology, two microwave antennas with a straight line of sight between them are utilized, ensuring no obstacles to disturb LOS. Therefore, this is utilised usually for achieving privacy. Here, frequency range of terrestrial system is specifically 4 GHz -6 GHz, and the information communication rate is often 1 Mb/s to 10 Mb/s.

However, major drawback of microwave signalling is that these may get affected due to bad weather, and specifically because of raining. Microwave communication can be used for long

distance transmission/reception of signals, and a lot of their uses are found in day-to-day lives. A few of their uses in terms of technology are mentioned in next section.

The following three categories fall into microwave communication:

- *Wi-Fi:*

Wi-Fi is one of the low power wireless transmission systems, which is utilized by different electronics devices such as smart phones and laptops etc. Under such scenario, a wireless router acts as a communication hub. Such networks permit subscribers to connect only within near proximity to a router. Wi-Fi is quite usual in the domain of networking services, which facilitates portability of communication devices. The range for Wi-Fi communication is around 30m from the location of router.

- *Mobile Communication System:*

The advantage of mobile networking is reflected by generation. A large number of subscribers communicate by using single frequency band through mobile equipments. Cellular as well as cordless devices are two examples of equipments that are making use of wireless signalling schemes. Particularly, cellular mobile communication devices have a much greater range of networks to cater a coverage, however cordless communication equipments are bounded to a limited range. Akin to GPS equipments, some communication phones are making use of received signalling waveforms from satellites for communication [2]. Antennas are required at base station, and the mobile station in order to allow the users to communicate with each other.

- *Bluetooth Technology:*

The major function of Bluetooth scheme is that it allows subscribers to access different electronic equipments for transferring information to a system without using wires. Cell phones may be connected to hands free earphones, mouses, and keyboards without utilising wires. By utilising Bluetooth equipment, information can be transferred from one wireless system to other system. This wireless scheme exhibits various functions, and this can be utilized usually in wireless communication scenario for data transfer up to 10 m range.

Because of the on the move connectivity of a wireless communication system, it is one of the most preferred system for communication. For this communication to take place, antennas are required at both transmitter and receiver side for successful communication. An antenna acts as a transducer

device to convert electromagnetic radiation in space into electrical currents or vice-versa at transmitter and receiver side.

Nowadays, since all devices for wireless communication need to be small and handy, the antennas required for such devices should also be smaller and compact. Microstrip antennas described in next section are small and easy to fabricate, and these are therefore preferred.

1.2 INTRODUCTION TO MICROSTRIP ANTENNAS:

Patch antennas can be fabricated easily, and have a low profile as well as low cost. Figure 1.1 shows a microstrip patch antenna [3], it has a dielectric substrate with $2 \leq \varepsilon_r \leq 12$. The dielectric substrate consists of pattern on one side and ground plane on other side of it. Microstrip patch antenna has radiating patch on one side and ground on other. Attached to patch, there is microstrip feedline that excites the patch with respect to ground.

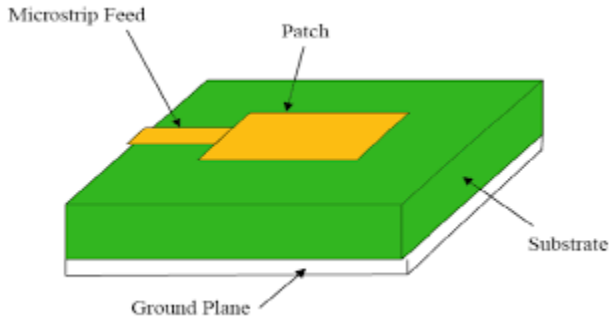

Figure 1.1 Design of microstrip patch antenna [3]

Thick size dielectric material with lower dielectric constant will provide good antenna performance. This gives improved efficiency as well as radiation pattern and also large operating BW. Microstrip antennas are smaller in size and operate at microwave frequencies.

1.2.1 Advantages of Microstrip Antenna:

- They operate at microwave frequencies, where traditional antennas are not feasible to be designed.
- This antenna type has smaller size, and hence will provide small size end devices.
- The microstrip based antennas are easily etched on any PCB and will also provide easy access for troubleshooting during design and development. This is due to the fact that microstrip pattern is visible and accessible from top. Hence, they are easy to fabricate and comfortable on curved parts of the device. Hence, it is easy to integrate MICs or MMICs.

- As the patch antennas are fed along centreline to symmetry, it minimizes excitation of other undersigned modes.
- Microstrip patches of various shapes e.g., rectangular, square, triangular etc. can be easily etched.
- These exhibit low fabrication cost, and therefore these may be manufactured at a large scale.
- They are capable of supporting multiple frequency bands (dual, triple).
- They support dual polarisation types viz. linear and circular both.
- They are light in weight.
- They are robust, when mounted on rigid surfaces of the devices.

1.2.2 Disadvantages of Microstrip Antenna:

- Some spurious radiations are present in different microstrip based antennas, like in printed dipole antenna, microstrip slot antennas as well as in microstrip patch antenna.
- This provides lower efficiency because of dielectric losses as well as conductor losses.
- This provides alleviated gain.
- It has higher level of cross polarisation radiation.
- It has lower power handling capabilities.
- It has inherently lower impedance bandwidth.
- The microstrip antenna structure radiates from feeds and other junctions points.

Apart from the disadvantages of microstrip patch antenna, they are a preferred choice in most wireless devices. Among microstrip patch antennas, many designs and geometries are available to offer a better performance; like slot shaped structures, fractal patches, and many more. Since fractal antennas allow multiple and lower frequency bands to be generated with small sized structures. They are a preferred choice.

1.3 FRACTAL ANTENNAS:

As a advanced field referred to as fractal-electrodynamics, it has considerably affected antenna theory, and has lead to the exploitation of geometry of fractals in science as well as engineering.

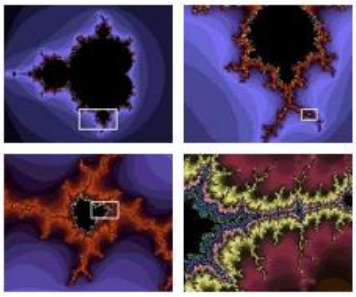

Figure 1.2 Mandelbrot depiction [4]

For fractals, there is a little extent of self-symmetric property, that is why it is difficult to define fractals mathematically. Generally, some key features are seen in fractals. The Mandelbrot [4] set, which is proper representation of this, is shown in above mentioned Figure 1.2. There are many fractal geometries available. Koch snowflake is one example of a fractal set. Figure 1.3 depicts the first few iterations of Koch Snowflake.

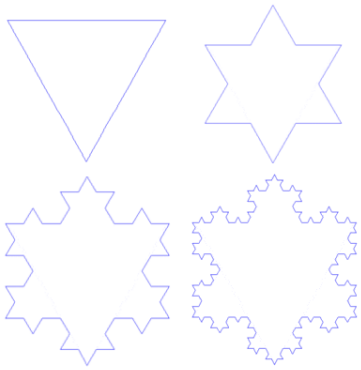

Figure 1.3 Koch snowflake pattern at iteration 0, 1, 2 and 3 [7]

In the total surface area, the length of the material can be maximised by designing a self-similar fractal antenna. Thus, compactness and wideband are key features of fractal antennas. A virtual network of capacitors and inductors is shown in fractal antenna, and is reason for different resources which arises. Presently, a number of cell phones utilise a Planar Inverted-F Antennas (PIFAs), that are small, low-profile, and are sensitive to both horizontal as well as vertical polarized radio waveforms. Its main disadvantage is narrow BW and lack of multiband nature. Fractal PIFAs are designed to tackle such issues, but its outcomes are quite promising.

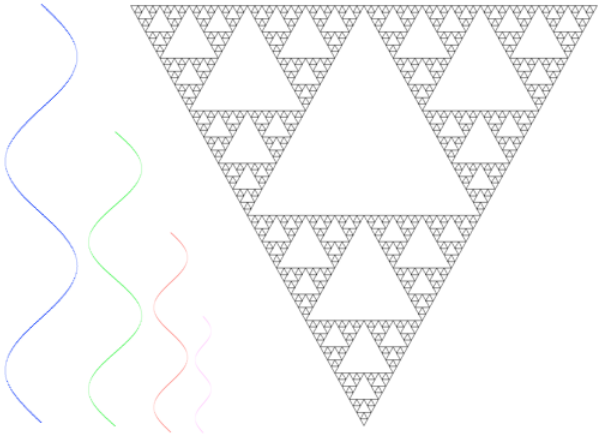

Figure 1.4 Resonances allowed for this geometry [5]

Figure 1.3 shows a triangular sierpinski gasket fractal upto four iteration, and Figure 1.5 shows a cantor set evolution.

Figure 1.5 Cantor set F-PIFA evolution [4]

1.4 FRACTAL MICROSTRIP ANTENNAS:

Nowadays, versatile circuit designs and compactness are required in this digital environment, thus development of fractal microstrip antenna is playing a vital role. Whether it is square, circular, or triangular, fractal microstrip antenna [5] increases the perimeter of initial geometry, and they are widely used for antenna miniaturization. Thus by decreasing the length of filters, antennas or any other EM device, the electric length of the device increases. These antennas give multiband frequency response, and exhibit miniaturization of microstrip patch antennas. Thus fractal geometry is quite significant in circuit designing for any microwave applications. Therefore, the investigation of escape-time fractals such as Mandelbrot sets is of substantial interest in communication standards, especially because of its unusual geometries, which enable the development of advanced circuit designs with enhanced performance.

For near millimetre wave application, Mandelbrot sets; and for distance communication, sierpinski [6] gasket fractal sets are explored for its utilisation in designing of microstrip patch antennas. The development of multiband and compact microstrip antennas is expanding because of Mandelbrot fractal geometries, being a wonderful exclusive choice for wireless and near millimetre-wave services, like in any 5G communication system as well as in the automotive industrial applications.

In order to excite these fractal antennas, four main feeding techniques are mentioned in the next sections.

1.5 FEEDING TECHNIQUES:

A microstrip patch antenna can be fed or electromagnetic energy can be transferred through many techniques. To modify the antenna input impedance matching for efficient working of antennas, feeding is very important. Most popular four feeding techniques are given below.

1.5.1 Microstrip Feed:

The microstrip feed line can be used to excite patch. This may be etched on same substrate, so as total configuration remains planar; this is an advantage of such feed. However, radiations from feed line is the disadvantage leading to increase in the cross-polar level. Photoetching is the process used to make microstrip feed on the substrate, which acts as a conducting strip. The spurious feed radiation is introduced, which limits the bandwidth as height of substrate is enlarged. Also millimetre- wave range leads to an increase in undesirable radiation. Figure 1.6 shows the geometrical configuration of microstrip line fed microstrip patch antenna [10].

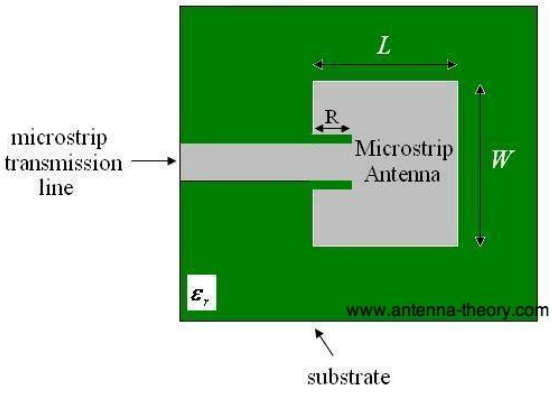

Figure 1.6 Microstrip feed [3]

1.5.2 Coaxial Feed:

Another name for coaxial feed is probe feed. In this feed, the centre conductor is solder to the patch. The coaxial feed can be placed according to the requirement on inner side of patch for matching to its input impedance. This appears as main benefit for this coaxial feed. This structure is not completely planar as the whole. Therefore to get it drilled in substrate, connector is extended outside the bottom ground plane. This makes the arrangement asymmetrical, thus leading to disadvantages of the coaxial feed. Figure 1.7 shows a coaxial feed antenna.

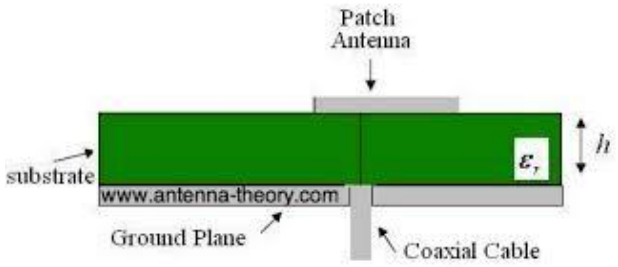

Figure 1.7 Coaxial feed [3]

1.5.3 Aperture Coupling:

Aperture coupling is another method for indirectly exciting a patch. Utilising an electric compact aperture or slot cut in ground plane, field is coupled from microstrip line feed to radiating patch (leading to less cross-polarization because of symmetry of the structure). Here, coupling aperture is often centred beneath patch. However, extent of coupling from feed line to patch is decided by shape, size as well as location of aperture. Moreover, slot aperture may either resonant or non-resonant. But, bandwidth is increased at the cost of increasing back radiations, because the resonant slot gives another resonance besides patch resonance. Thus, a non-resonant aperture is normally preferred. Due to low errors in alignment of various layers, performance is relatively insensitive. The substrate parameters of two layers may be selected independently for optimum antenna performance akin to the EM coupling technique. Main advantage of this feeding is that this provides increased bandwidth. Figure 1.8 shows the aperture coupled microstrip patch antenna.

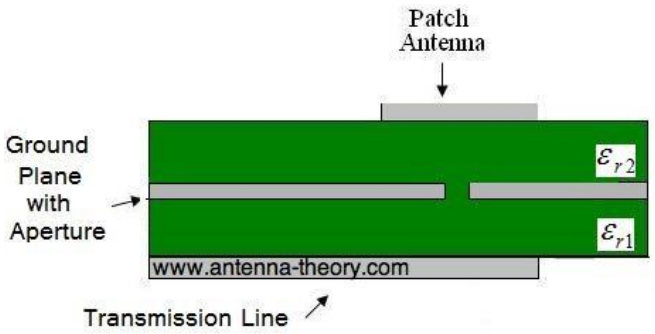

Figure 1.8 Aperture coupling [3]

1.5.4 Proximity Coupling:

In this category of feed between patch and ground plane, the feed line needs to be placed, which is separated by two dielectric media. Due to enhancement of overall substrate thickness belonging to microstrip antenna, the bandwidth of antenna increases. Here, selection between two different dielectric media, first for patch and second for feed line to optimize individual performance as well as for elimination of spurious feed-network radiation are the some advantages of this feeding technique. The main disadvantages of this feed are that overall thickness of antenna gets increased, and that two layers are required to be aligned appropriately. Figure 1.9 demonstrates a proximity coupled microstrip patch antenna.

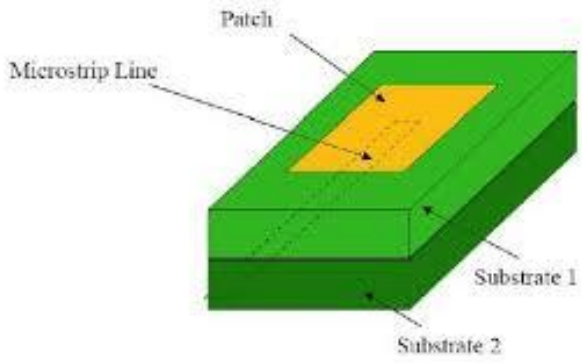

Figure 1.9 Proximity coupling [3]

1.6 MATHEMATICAL ANALYSIS OF APERTURE COUPLED MSA:

Among the four popular feeding techniques described above, aperture coupled is the most preferred feeding. Probe-fed microstrip patch antennas have an abundant literature on the theoretical analysis. The brief review of the most popular method i.e., transmission line method is discussed in the next section.

1.6.1 Transmission Line Model:

Earliest of all the methods is the transmission line model, but the drawback is that this exhibits less accurate outcomes, and this is also lacking in versatility. The two slots of width W, height h are separated by lower impedance transmission line of length L. Here, substrate and air are the two dielectrics of the lines of non-homogeneous microstrip. Moreover, fields along the edges of patch undergoes fringing due to the finite length as well as width of microstrip patch antenna. Here, height of substrate as well as dimensions of patch determine extent of fringing. The resonant frequency of patch antenna influences fringing, and that's why it's an important factor in account to the calculations.

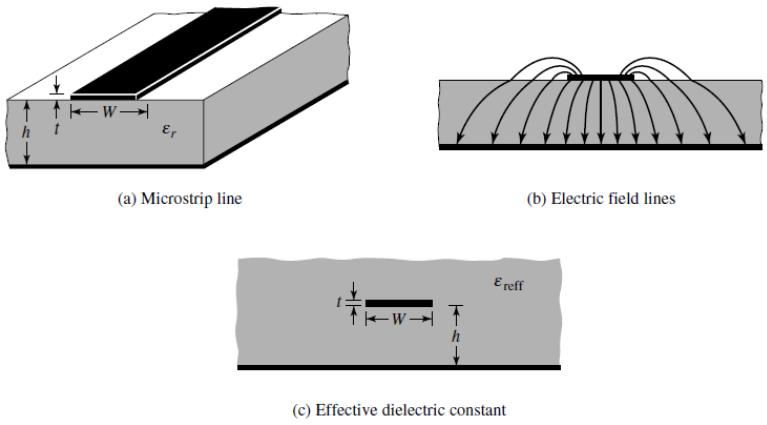

Figure 1.10 Microstrip line and its electric field [25]

As observed in above figure, a few electric field lines exist in air, but a number of it reside inside substrate. Hence due to fringing effects, in comparison to physical dimensions of microstrip line, the electrical dimensions look wider. As the phase velocities are non-matching in air and substrate, such transmission line can't favour true transverse electromagnetic (TEM) mode of propagation. The quasi-TEM mode will be dominant mode in transmission. In order to account for fringing as well as wave propagation in line, an effectual dielectric constant ε_{reff} ought to be attained. Here, value of the actual dielectric constant ε_r of the substrate would be nearer to value of ε_{reff}. However, electric dielectric constant ε_{reff} exhibits range of $1<<\varepsilon_{reff}<<\varepsilon_r$ for air dielectric substrate. Moreover, the effectual dielectric constant ε_{reff} is dependent on frequency. Equation for ε_{reff} is provided below

$$\varepsilon_{eff} = \frac{\varepsilon_r+1}{2} + \frac{\varepsilon_r-1}{2}\left(1 + 12\frac{h}{W}\right)^{\frac{1}{2}} \quad 1.1$$

Where, ε_{reff} = Effective dielectric constant

ε_r = Dielectric constant of substrate

h = Height of dielectric substrate

W = Width of patch.

As fringing fields cause patch to look electrically wider, the length of patch gets elongated on every side by a distance **Δ**L.

An approximate relation is:

$$\frac{\Delta L}{h} = 0.412 \frac{(\varepsilon_{reff}+0.3)(\frac{W}{h}+0.264)}{(\varepsilon_{reff}-0.258)(\frac{W}{h}+0.8)} \quad 1.2$$

Due to the extension of **Δ**L, effective length becomes:

$$L_{eff} = L + \Delta L \quad 1.3$$

Resonant function of the structure is a function of its length given by:

$$f_r = \frac{1}{2L\sqrt{\varepsilon_r}\sqrt{\mu_0\varepsilon_0}} = \frac{v_0}{2L\sqrt{\varepsilon_r}} \quad 1.4$$

v_0 = speed of light

The design procedure assumes that the resonant frequency, dielectric constant and substrate height are known.

- First step is to specify the known resonant frequency f_r, the substrate height h, and dielectric constant ε_r.
- Next is to determine width of patch by utilising expression given below

$$W = \frac{1}{2f_r\sqrt{\mu_0\varepsilon_0}}\sqrt{\frac{2}{\varepsilon_r+1}} = \frac{v_0}{2f_r}\sqrt{\frac{2}{\varepsilon_r+1}} \quad 1.5$$

- Next is to determine the effective dielectric constant using equation 1.1
- Once W has been calculated, **Δ**L is also calculated.
- Further, actual physical length of patch is obtained by using

$$L = \frac{1}{2f_r\sqrt{\varepsilon_{reff}\sqrt{\mu_0\varepsilon_0}}} - 2\Delta L \quad 1.6$$

In order to achieve a wideband performance from a conventional fractal microstrip patch antenna with multiband performance, a technique called stacking is used. In this method, multiple layers of dielectric substrate need to be attached or stacked one above the next, such that one is driven patch, and it has multiple parasitic patches above it [18].

These parasitic patches can be of same or varying dimensions, as the driven patch is also the dielectric substrate, which can be of same or varying dielectric constants. Based upon the literature survey carried out in the field of research work, stacked aperture coupled microstrip patch antennas, presented in this thesis report deals with the design, fabrication, testing and performance evaluation of stacked aperture coupled microstrip patch antenna. These antennas are designed for a multiband performance, and their bandwidth enhancement is achieved by using stacked antennas of same size as driven patch.

In order to carry out the research work, around fifty research papers were found out. These are mentioned in subsequent chapters.

1.7 RESEARCH GAP:

An extensive literature survey is carried out in chapter 2 that deals with design as well as development of different categories of fractal antennas for UWB applications. A few research gaps that were identified are:

- Not much work is available in the literature that concentrate on multilayer fractal antenna, which can lead to an improvement in bandwidth.
- Using aperture coupled feeding with fractal microstrip antennas is also an open area of research.
- The aperture in ground layer can be made defective to improve the operational bandwidth, and hence achieve an operational ultra-wideband.
- Stacked sierpinski gasket fractal antennas with driven and parasitic patches of same dimension can be designed, and hence to achieve peak gain of 5.40 dBi.

On the basis of the literature review and the research gaps found out; following objectives were defined for the current research work.

1.8 THESIS OBJECTIVE:

- To design and simulate a triangular sierpinski gasket fractal antenna with aperture coupled feed for multiband operations.
- To analyze stacked triangular sierpinski gasket fractal antennas with three main types of geometries:
  - **a)** Stacked sierpinski gasket fractal antenna with driven and parasitic of same dimension.
  - **b)** Stacked siperpinski gasket fractal antenna with parasitic patch smaller than driven patch.
  - **c)** Stacked sierpinski gasket fractal antenna with driven patch smaller than the parasitic patch.
  - **d)** Compare the performance of all three geometries.
- To design, fabricate and test a triangular sierpinski gasket bow-tie fractal antenna with same dimensions as that of driven and parasitic patch.
- To design fabricate and test a diamond shaped sierpinski gasket fractal antenna with driven and parasitic patches of same size.

1.9 THESIS ORGANISATION:

The thesis is divided into following chapters:

- Chapter 1: Presents an overview of wireless communication, microstrip patch antennas, and fractal antennas and the objectives of research work are also defined in this chapter.
- Chapter 2: Presents the literature survey.
- Chapter 3: Presents the designing and simulation of a triangular sierpinski gasket fractal antenna with aperture coupled feed for multiband operation, and a comparative analysis of stacked and unstacked structures.
- Chapter 4: Presents the designing and simulation of an unstacked and stacked diamond shaped sierpinski gasket fractal microstrip antenna.
- Chapter 5: Presents the fabrication and testing of stacked bow-tie sierpinski gasket fractal antenna with driven and parasitic patches of same dimension, and stacked diamond sierpinski gasket fractal microstip antenna using PCB technology and VNA respectively. Comparative study of simulated results and measured results is done.
- Chapter 6: Concludes research work carried out in the presented thesis, and a small discussion on future scope is also given.

CHAPTER-2

LITERATURE SURVEY

The current chapter describes the literature survey of fractal antennas, aperture coupled antennas and stacked aperture coupled antennas. This chapter explores study of aperture coupled microstrip antennas, stacked structures, use of partial ground and defective ground for ultra-wide band applications.

C. A. Balanis's main objective in [24] was to provide details about fundamental principles of antenna theory, and employ these for analysis, design, measurements of antenna. Most elementary antenna properties like gain, directivity, radiation efficiency, impedance, surface current as well as polarization have been discussed in brief. Discussion on various schemes as well as systems utilised in near-to-far field measurements and transformation is carried out in this article.

V. P. Patil in [25] presented a rectangular MPA with two slots embedded diagonally on its side surface as the effectual scheme for enhancement of bandwidth of the patch antenna to meet prerequisites for wireless standards. The suggested antennas was simulated as well as analyzed using GENESYS software. Here, antenna characteristics, such as VSWR, input impedance and S_{11} parameters are analyzed. The simulated results for the proposed antenna gives impedance bandwidth of 311 MHz, whereas fabricated antenna gives the bandwidth of 286 MHz.

J. P. Gianvittorio *et al*. in [26] gave the brief study on fractal antennas and its various geometries. Fractal antennas with self-similarity property had same possibility as that of conventional MPA for accomplishing multi band behavior by using multiple radiating elements or relatively loaded patch antennas. The self-similar nature provided similar surface current distributions for various resonating frequencies, and space filling property of fractal antenna increased the electrical length of the radiating element.

A. Kaur in [27] presented the design and testing of a semi-spiral G-shaped small configuration using CST MWS'10 software for WLAN, WiMAX as well as U-NII band standards. To achieve multi-frequency and broadband behaviour, resonant slots in patch with aperture coupled feeding technique was considered. Testing of antenna was done using VNA. A gain of 4.5 dB was achieved for all the three applications.

A. Kaur *et al.* in [28] gave the complete review of current developments in the domain of fractal antenna engineering. A brief description about fractals with its designs and algorithms used for optimization and work done in this field of fractals were discussed.

A. Kaur *et al.* in [29] proposed a aperture coupled stacked sierpinski gasket fractal antenna with DGS for UWB and WLAN applications. Antenna was designed as well as simulated by utilising CST MWS'10 software. Dual wideband behaviour with a BW (bandwidth) of 630 MHz and 400 MHz was observed. Gain of 5.85 dB and 9.5 dB for two bands was achieved. Measured outcomes were in good agreement with simulated ones.

Z. U. Islam *et al.* [6] show that sierpinski monopole fractal antenna was operational in S and C bands i.e., for dual bands. For radiation of antenna in two frequency bands, fractalization was performed upto second order. The optimisation of antenna for desired bands was done for various dimensions of ground plane and feed line of antenna.

S. Neha *et al.* [7]: In this paper, as fractal iterations increase, perimeter of patch increases and effective area of antenna increases with enhanced multiband application. The radiator was found to be resonant at higher number of frequencies. This gave multiband properties to fractal geometry antenna with directive patterns**.** The resonant frequency increased with an elevation in number of iterations. Multiband behaviour was attained, as the number of iterations were elevated. Therefore, Koch snowflake antenna is a nice example of the characteristics of fractal incremental boundary patch antennas.

N. S. Dandgavhal *et al.* [8]**:** The designed antenna in this paper was likely to operate in four frequency bands for various services. First frequency band was 1.41 GHz - 1.65 GHz, which covers GPS operating band, second band was 3.41 GHz - 3.81 GHz and third was 5.41 GHz - 5.80 GHz. Both bands cover WiMAX operational range. However, 7.75 GHz - 8.13 GHz was the last band that covered X-band. Here, X-band was utilised in radar applications.

M. T. Islam *et al.* [9]: This paper presented an antenna of compact size of (21.44x23.53) mm^2, which achieved a bandwidth of 8.51 GHz (3.49-12 GHz). After designing a tapered slot ground with rectangular slotted patch, it covered a wider bandwidth and enhanced coupling between rectangular slot and feed line. By varying slot size as well as shape, better impedance matching may be obtained.

N. Cohen in [30] applied fractal geometry to conventional antenna elements, which resulted in size miniaturization of antenna, improved bandwidth, better input impedance and multiband resonant frequencies without changing the physical length of antenna. Merits as well as demerits and its application in the domain of wireless signal transmission systems were discussed.

L. C. Ping *et al.* [10]: In this paper, UWB microstrip patch antenna was presented, which covered a bandwidth between 1.78 GHz-11.13 GHz (9.35 GHz). By using slot, impedance bandwidth was better than unslotted antenna. The variation of the antenna parameters explored did not have effect on return loss S_{11} of antenna output.

A. Gorai *et al.* [11]: The antenna in this paper was radiating in Bluetooth frequency band centered at 2.4 GHz and exhibited band rejection at 5.5 GHz. A Koch fractal boundary was embedded over the hexagonal-shaped radiator to enhance input impedance matching of antenna at larger frequencies. The antenna size was 18.5 × 39 mm, and it was compatible to dongle equipment with radiating portion being 18 × 8.7 mm^2.

E. E. M. Khaled *et al.* [12]: The paper proposed a design of proximity fed planar annular slot antenna for UWB applications. The antenna covered a bandwidth from 2.82 to 10.74 GHz, while demonstrating quite sharp band-rejection output at 5.51 GHz.The antenna showed constant gain, high efficiency and omni-directional field pattern.

A. S. W. Ghattas *et al.* [13]: The proposed antenna had a size of 20x20x1.5 mm^3. A proximity fed UWB antenna having four notched bands at 3.5, 3.9, 5.25 and 5.9 GHz to evade interference was presented, which covered a frequency band ranging 1.9 GHz to 10.3 GHz with omni-directional radiations. To attain the needed four band notches, the etched slots as well as slits in the ground plane are incorporated.

K. Ruchandani *et al.* [14]: Authors present a design with a coplanar waveguide fed printed octagonal aperture antenna having a rejection frequency band of 5-6 GHz (suppresses WLAN band), which is attained by etching H shaped slot from back patch of traditional UWB antenna. It had a compact size of 30x30 mm^2, and covered the whole UWB from 2.8 GHz to 10.7 GHZ.

A. S. W. Ghattas *et al.* [15]: This paper presented an antenna with a cedar tree-shaped cut through patch having an overall size of 20x20x1.5 mm^3 and four notched bands at 3.5, 3.9, 5.25 and 5.9 GHz to evade interference. To attain needed four band notches, the etched slots as well as slits in

ground plane were incorporated. This reported antenna provided wideband performance in the frequency band 3 to 11.7 GHz.

R. A. Abdulhasan *et al.* [16]: This paper presented a compact size antenna having U as well as J shaped slots in patch for rejection of WiMAX and WLAN. It had a better performance over the whole frequency band (3.1 GHz to 10.6 GHz) except WiMAX (3.15-3.7 GHz) and WLAN (5.15-5.85 GHz) notched frequency band.

S. Sarkar *et al.* [17]: This correspondence presented a stacked bow-tie antenna with bandwidth (6-11 GHz). Proximity coupling helped in reduction of feed line radiation. By utilising the parasitic patches as well as tuning stubs, microstrip antenna had been transformed into a multiple resonant configuration. All the measurements had been carried out inside the anechoic chamber.

A. Agarwal *et al.* [18]: The paper presented a dual band stacked microstrip antenna array for WLAN. Stacking of patches was performed to attain dual band. The input impedance was too sensitive towards separation distance between two conductions. The slits as well as slots were cut on upper as well as lower patch to excite higher number of resonant frequencies near to stacked patch frequencies. It covers a bandwidth of 228.3 MHz from 3.63 to 3.86 GHz and 235 MHz from 5.15 to 5.38 GHz.

L. C. Ping *et al.* [10]: In this paper, UWB microstrip patch antenna was presented, which covered a bandwidth between 1.78 GHz-11.13 GHz (9.35 GHz). By using slot, impedance bandwidth was better than unslotted antenna. The variation of the antenna parameters investigated doesn't exhibit effects on return loss and on S_{11} of antenna response.

J. Y. Sze *et al.* [19]: The proposed antenna had a compact size 25x15 mm^2 and had a bandwidth 3.06-16.5 GHz. To produce enhanced impedance matching with VSWR ≤ 2, the single strip of CPW needs to be projected into aperture to form a stub. An additional grounded rectangular patch could result in required notched band within ultra-wide band.

M. Khan *et al.* [20]: This paper presented an antenna in UWB region with large bandwidth with high and steady gain. It had a simulated impedance BW of 57.8% centred on 7.3 GHz with peak gain of 6.8 dB. Change in arm angle V-slot showed trade-off between quality of VSWR as well as BW.

C. Elavarasi *et al.* [21]: This paper presented the CSRR loaded sierpinski fractal antenna for multiband services. The simulated outcomes offered three operational bands, covering C band at

5.72 GHz, Ku band at 14.3 GHz as well as 16.06 GHz. However, size of CSRR loaded Gasket antenna was 14 mm x 12 mm x 1.6 mm^3 printed on FR4 substrate.

S. Yadav *et al.* in [41] presented a Koch curve fractal antenna for UWB services. Different iterations for designing proposed antenna was discussed. An omni-directional radiation pattern with acceptable gain was obtained. It was fabricated on FR4 substrate material possessing dimensions 33.5×28.5×1.6 mm^3. It covered C band applications (2.8-6.4 GHz) and WiMAX (3.4-3.69 GHz).

S. Jagadeesha *et al.* in [38] outlined a multiband fractal antenna design. A plus shaped microstrip antenna was designed and simulated using IE3D software. Antenna radiated at multi resonant frequencies. Using fractal antennas, 82.6% of size reduction was achieved. A better match between the simulated results as well as experimental outcomes was noted.

A. Bisht *et al.* in [32] presented a novel cup shape slotted antenna for UWB applications. Proposed design contained a radiating patch with cup shape slot in it. An ultra-wideband ranging from 2.45-10.9 GHz was achieved. Simulated outcomes and measured outcomes were further studied.

A. Azari in [31] designed an octagonal fractal antenna for achieving multiband, broadband and UWB applications. The simulation as well as optimization were carried out by using CST MWS. Proposed antenna covered a frequency range of 10-50 GHz with 40 GHz bandwidth resulting in a super wideband antenna. Gain and radiation pattern were also discussed.

D. M. Pozar *et al.* in [47] described the design and fabrication process of a circularly polarized aperture coupled antenna for GPS applications. Antenna operated at two resonant frequencies of 1227 MHz and 1575 MHz. Further, the suggested antenna was tested and outcomes were compared with simulated ones.

M. Singh *et al.* in [40] presented the design and fabrication process of microstrip aperture coupled patch antenna using 0.762 mm and 0.508 mm thick substrates at 10 GHz frequency. The design was optimized by varying antenna parameters using a 3D electromagnetic simulator. Further, simulated and measured results were studied. A gain of 6.21 dBi at 10 GHz was achieved, and it was suitable for X band communication systems.

A. Sundaram *et al.* in [52] proposed a Koch folded-slot antenna iterated up to 2 iteration level. The simulation results for all three iterations were studied. It was observed that a better impedance bandwidth was achieved, as the iteration level was increased. Return loss achieved for all three

iterations was 40 dB, 34 dB and 42 dB with a bandwidth of 1.211 GHz, 0.4 GHz and 0.34 GHz respectively.

C. P. Baliarda *et al.* in [51] described the unique geometric properties of fractal. The behaviour of Koch curve monopole antenna was analyzed numerically and experimentally. As the level of iteration on proposed antenna was increased, Q factor of antenna approached the fundamental limit for small antennas.

R. G. Hohlfeld *et al.* in [50] described that the self-similarity property of fractal antenna and original symmetry were key geometric constraints in determination of frequency independence property of antenna. Frequency independence was not dependent on self-complementary property of fractal antenna, but it helped in smoothing out the impedance variations.

C. Puente *et al.* in [43] presented a model on sierpinski fractal antenna. The model was designed and simulated to operate at multiple frequency bands. The characteristics of suggested antenna were investigated with respect to parametric variations of simulated antenna. The prototype was tested and fabricated.

K. J. Vinoy *et al.* in [42] derived the approx. formulation for known resonant frequency of a Hilbert curve fractal antenna. Hilbert curve fractals because of their self-similar structures could be utilised as minor resonant antennas, which are beneficial in VHF/UHF signal transmission applications. Formula derived in this article could be further investigated to attain antenna design expressions (mathematical) for specified resonant frequencies.

A. Aggarwal *et al.* in [34] designed a Pythagoras tree fractal antenna with CPW feed technique. The proposed antenna was designed to resonate at two frequencies of 2.4 GHz for WLAN/WiMAX applications and 3.5 GHz for WiMAX/ ultra-wide band applications. Fabricated antenna shows a good match with simulated antenna.

D. H. Werner in [48] described fractal antenna engineering, which emphasized in two areas. Here, one area dealt with design as well as analysis of fractal antenna elements. However, other one dealt with application of fractal concept to the development of antenna arrays. Here, fractals are composed of many self-similar copies of the base shape antenna. Exclusive characteristics of fractal have been utilised to define the fresh class of antenna elements for multiband and wideband operation, and that were compact in size.

Based upon the literature review carried out, a few research gaps were found out and hence a few objectives for the current research work were defined. These are mentioned in chapter 1, and the further chapters in this thesis deal with each objective and the procedure of carrying out each of those. The results are also summarized in each chapter accordingly.

CHAPTER-3

DESIGN AND SIMULATION OF A BOW-TIE SIERPINSKI GASKET FRACTAL ANTENNA FOR MULTIBAND OPERATIONS AND A COMPARITIVE ANALYSIS OF UNSTACKED AND STACKED STRUCTURES

This chapter describes design as well as simulation of a sierpinski gasket fractal antenna using aperture coupled feeding. This antenna is converted to a bow-tie shaped antenna by joining two sierpinski gasket fractal at the apex. Stacking of the bow-tie sierpinski gasket fractal antenna is then done to achieve a good bandwidth at the desired bands. A comparative analysis of stacked and unstacked fractal antenna geometries is then done. Four fractal antenna geometries namely, an aperture coupled bow-tie antenna, a scaled aperture coupled bow-tie with same dimension on upper and lower patch, a stacked bow-tie geometry with smaller upper patch and larger lower patch, and a stacked geometry with larger upper patch and smaller lower patch with bow-tie antennas for both stacked layers are studied and analysed. The overall size of the designed antenna is 57.84x57.84x4.815 mm^3 for all the four geometries. The ground used for an unstacked geometry is DGS i.e., defected ground slot and ground used for stacked geometry is a partial ground. The effect of both types of ground have been shown and studied. The submitted antenna results for all the four geometries are analysed as well as studied in terms of impedance bandwidth, broadband gain and VSWR. Here, antenna geometries and outputs are discussed in the next section.

3.1 UNSTACKED BOW-TIE STRUCTURE:

In this section, a triangular sierpinski gasket fractal aperture coupled antenna that is joined at the apex to form a bow-tie antenna is developed as well as simulated by utilising CST MWS V'17. The simulation outcomes are analysed in terms of return loss, BW, gain as well as current distribution.

3.1.1 Antenna Geometry:

The antenna geometry has three layers. The topmost substrate layer has a metal patch on it i.e., of a bow-tie pattern formed by joining two triangular sierpinski gasket fractals at the apex. The middle layer is metallic ground, which is 0.035 mm in height having cross shaped and

triangular shaped defects in it. The lower layer is a substrate; and at its bottom, a feed line printed up to the centre of the patch that has a stub of length λ/4 attached to it.

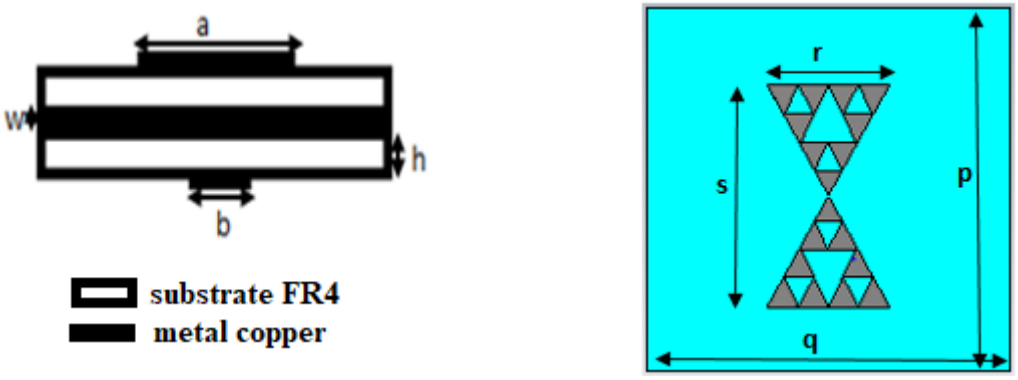

(a) (b)

Figure 3.1 (a) Front view of unstacked antenna, (b) Top view of unstacked antenna

The bow-tie patch has two triangles joined at the apex. Each triangle is subjected to two iterations, so as to make a sierpinski gasket individually of 2nd order. The design equation used to get a resonance of 4.31 GHz from the antenna input is mentioned in equation 3.1

$$f_{m,n,1} = \frac{2c}{3ae_{ff}(\varepsilon_{reff})^{\frac{1}{2}}}(m^2 + mn + n^2)^{\frac{1}{2}} \quad 3.1$$

$$a_{eff} = a + h(\varepsilon_r)^{-\frac{1}{2}} \quad 3.2$$

$$\varepsilon_{eff} = \frac{1}{2}(\varepsilon_r + 1) + \frac{1}{4}(\varepsilon_r - 1)(1 + \frac{12h}{a})^{-\frac{1}{2}} \quad 3.3$$

Where, ε_r = dielectric constant

a_{eff} = affective side

h = height of the substrate

m, n = TEM modes

The Figure 3.2 demonstrates top view of unstacked bow-tie antenna ground having defects in it. At the centre of the ground, a plus shape defect is made to increase the impedance matching. Afterwards to improve the bandwidth, a bigger triangle of side 27.5 mm at the left hand side

of the ground is cut, and a small inverted triangle of side 4 mm just below the plus shape is cut to get the desired results.

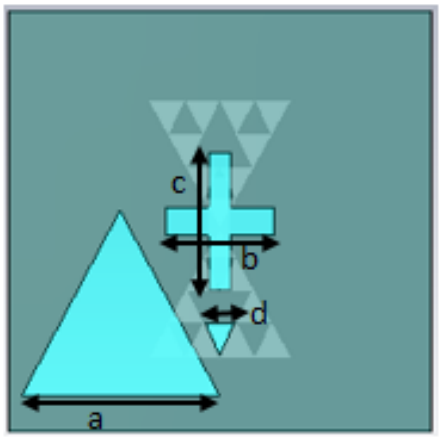

Figure 3.2 Defective ground of unstacked bow-tie antenna

The various antenna parameters of front and top view of antenna with their parametric values are discussed below:

Table 3.1 Dimensions of unstacked antenna

Parameters	**Dimensions(in mm)**
a	19.5
b	3
h	1.57
w	0.035
p	57.84
q	57.84
r	19.5
s	33.6
a(side of big triangle)	27.5
b(length of horizontal slot)	15
c	19
d	4

3.1.2 Simulation Results:

The antenna design discussed above is simulated by utilising CST microwave studio version 2017. Simulation results in terms of impedance bandwidth, current distribution and gain are presented in the next subsections.

3.1.2.1 Impedance Bandwidth:

The proposed antenna is a sierpinski gasket fractal antenna optimised upto 2nd iteration, and then converted into a bow-tie. Figure 3.3 shows S_{11} (dB) of the antenna. This stage is considered as the optimised one i.e., the 2nd iteration with a scaling factor of 1/3.

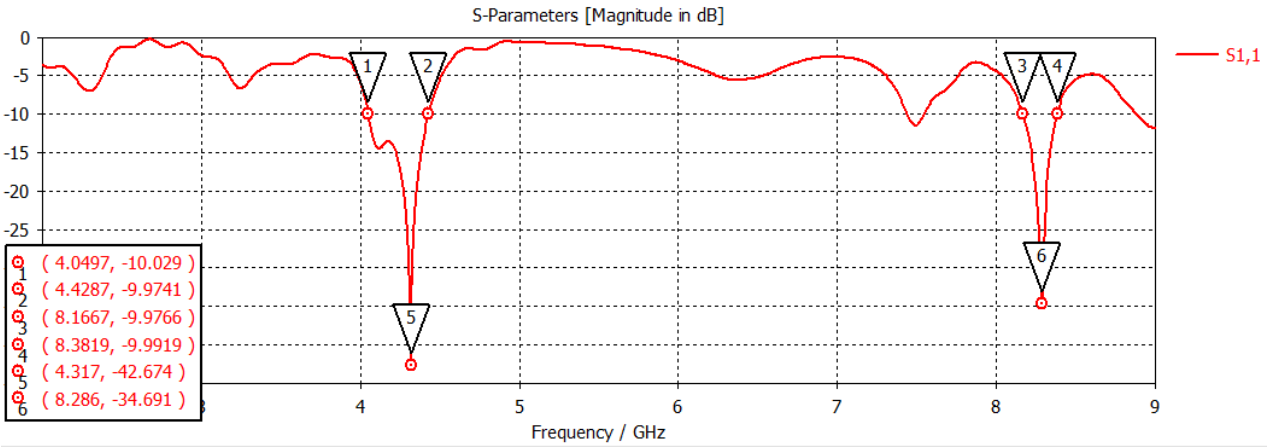

Figure 3.3 S_{11} plot of unstacked bow-tie antenna

3.1.2.2 Broadband Gain:

The overall broadband gain of sierpinski gasket fractal antenna is shown in Figure 3.4 that shows a peak gain of 5.18 dBi at 4.44 GHz and average gain of 4 dBi for the entire band. A good gain antenna can be used for long range wireless applications.

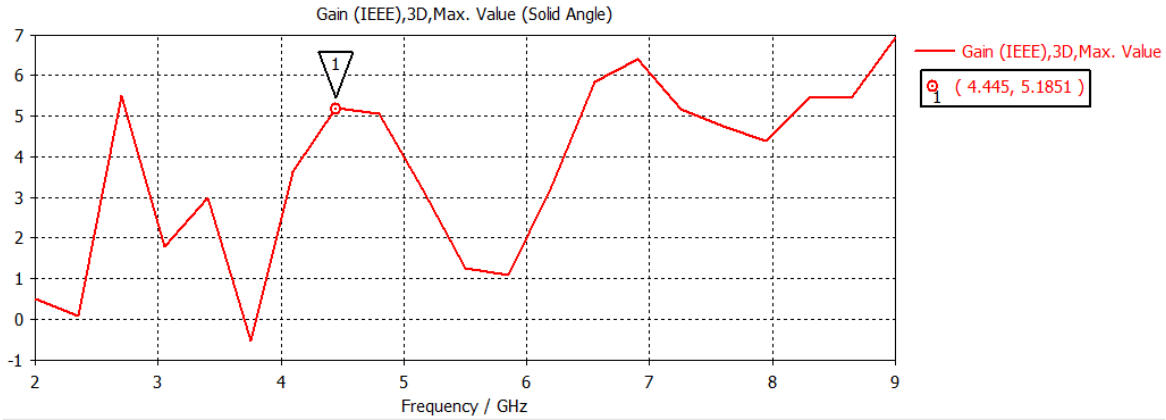

Figure 3.4 Overall broadband gain of unstacked bow-tie antenna

3.1.2.3 Radiation pattern:

Figure 3.5 shows the 3D plot at the frequency 4.31 GHz that shows a peak gain of 5.928 dB approx. The radiation efficiency and total efficiency are also mentioned in the Figure 3.5. Figure 3.6 shows polar plot of the unstacked bow-tie antenna at 4.31 GHz frequency. Figure 3.6 shows that the antenna has a major lobe direction along 145 degree and half power beamwidth of 57.2 degrees.

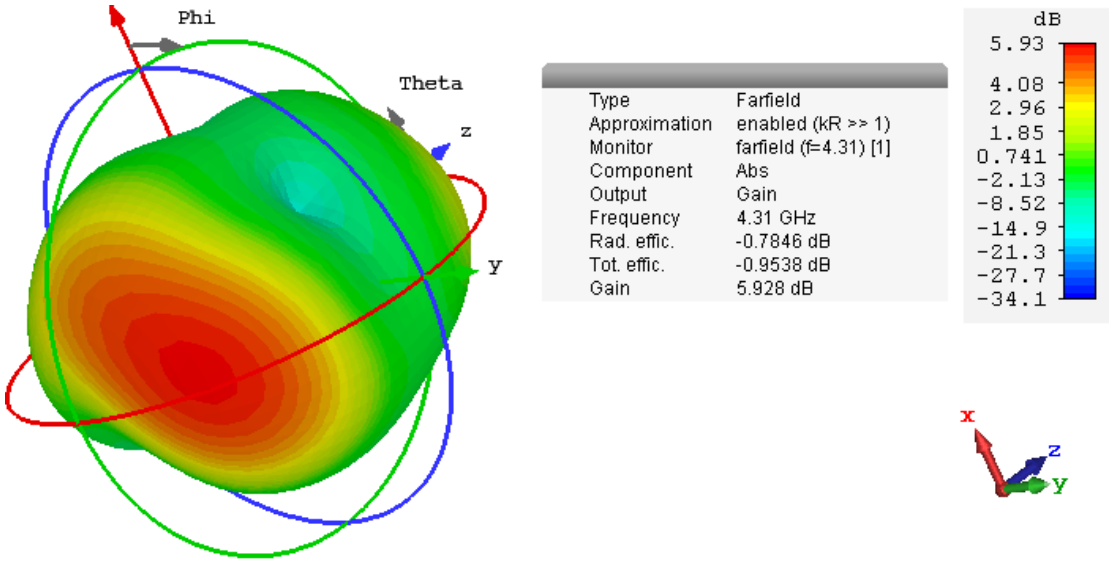

Figure 3.5 Radiation pattern of unstacked bow-tie antenna

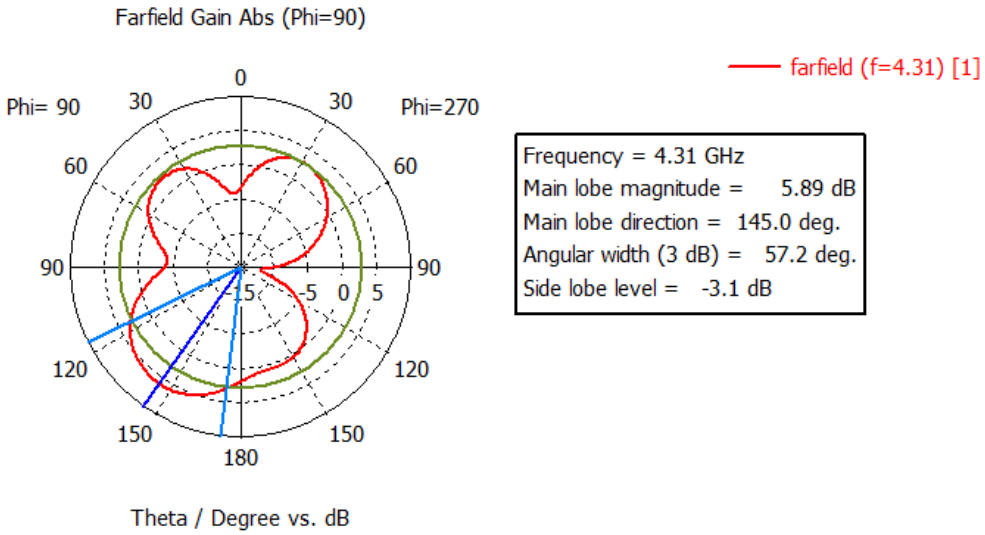

Figure 3.6 Polar plot of unstacked bow-tie antenna

3.1.2.4 Surface current distribution:

Figure 3.7(a, b) shows surface current distribution of ground for resonant frequencies 4.31 GHz and 4.23 GHz, when antenna is excited using microstrip feedline in the software. For frequency

of 4.23 GHz, the maximum current flows through the upper part of the plus slot and the smaller inverted triangle. Figure 3.7(c, d) illustrates magnitude of current distribution of patch at frequencies 4.31 GHz and 4.23 GHz. The intensity of current is more at the upper triangle of the patch than that to at the apex. Figure 3.7(e, f) demonstrates surface current distribution of strip line at frequencies 4.31 GHz and 4.23 GHz. The strip line have a stub, which really affects the magnitude of the current, and has the maximum current density at the stub.

Hence, it can be concluded that upper triangle of the bow-tie patch, and upper part of the plus slot and feedline are responsible for resonating lower resonant frequency of 4.23 GHz.

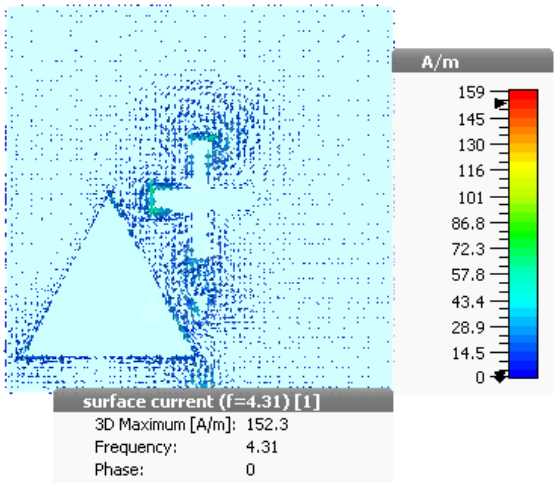

(a)

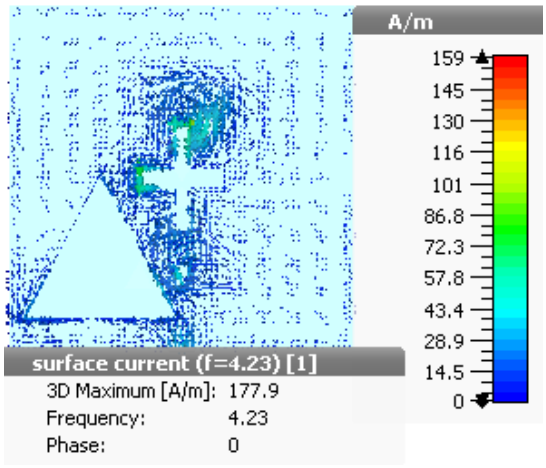

(b)

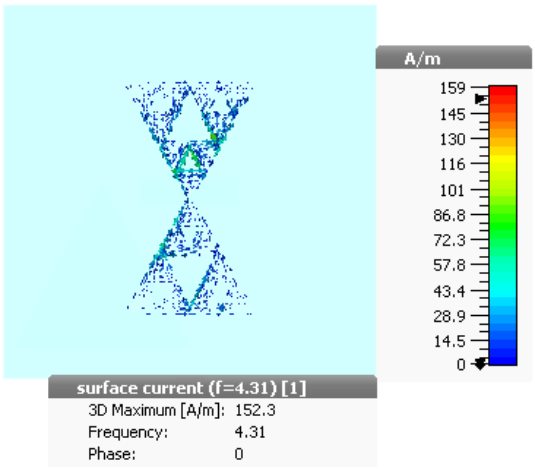

(c)

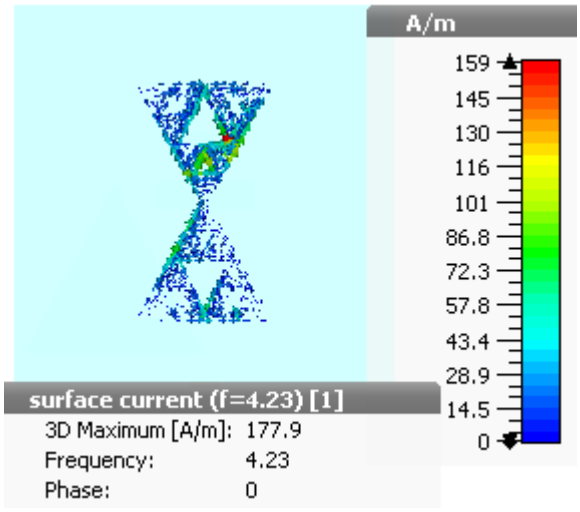

(d)

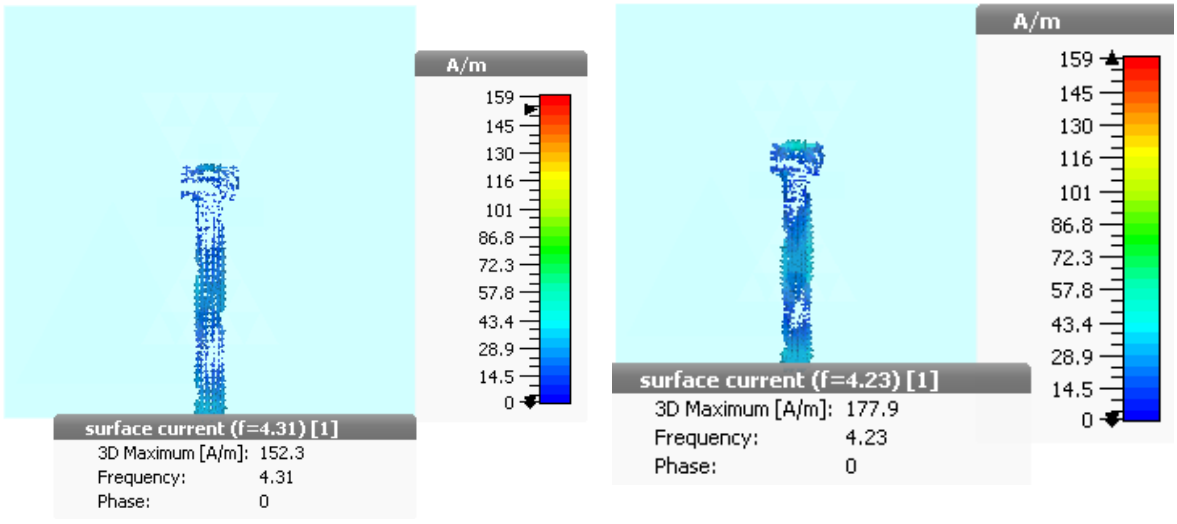

(e) (f)

Figure 3.7 Surface current distribution of presented antenna at resonating frequencies (a, c, e) 4.31 GHz (b, d, f) 4.23 GHz

3.1.3 Wireless Application Covered By Proposed Antenna:

The proposed antenna operates in the frequency band from 4.04-4.49 GHz and 8.16-8.38 GHz with bandwidth of 380 MHz and 270 MHz, which enables antenna to opertate over ultra-wide band (5.3-9.28 GHz), Radio Astronomy Band (5.01-5.03 GHz), as well as IEEE 802.11a WLAN applications (5.15 to 5.825 GHz).

The literature survey done on stacked micostrip patch leads to a conclusion that these antennas can be used to enhance the bandwidth of operation. Next section presents the stacking of Bow-tie antenna to improve the bandwidth of operation.

3.2 STACKED WITH SAME ACTIVE AND PARACITIC PATCH:

An aperture coupled sierpinski gasket fractal antenna is designed, which has a bow-tie like patch. Moreover, dimensions of both the active and parasitic patch are same. The main aim to switch from simple structure to stacked structure is to get multiple resonances and to achieve a good bandwidth. The two patches on the FR4 substrate layers are responsible for radiation and getting resonances at higher and lower frequency ranges. At the bottom of the FR4 substrate a feedline with stub of λ/4 length is used. With stacked structure, partial ground is used to get better results, which is sandwiched between two FR4 substrate layers. A plus slot has been cut in partial ground, which facilitates more impedance matching. CST microwave studio version 2017 has been utilised to design antenna and obtain the simulated results with assumption of perfect boundary conditions. The designed antenna resonates at lower frequencies 3.82 GHz, 4.1 GHz, 4.45 GHz and higher frequency 6.03 GHz. The bandwidth achieved is of 80 MHz

(3.86-3.78 GHz), 90MHz (4.14-4.05 GHz), 440 MHz (4.79-4.35) and 330 MHz (6.17-5.83GHz), which is used for short range Wi-Fi, wireless broadband and some cordless telephone.

3.2.1 Antenna Geometry:

The stacked bow-tie microstrip antenna presented here has three layers of FR4 substrate. The bottom most substrate of height 1.57 mm have a feed line of height 0.035 mm with a λ/4 stub below it. After that a layer of ground, above that another layer of substrate having bow-tie patch on it. And the upper most layer on this patch is another substrate of same height having parasitic patch above it of same dimension of active patch below. The front perspective of antenna is shown in figure below.

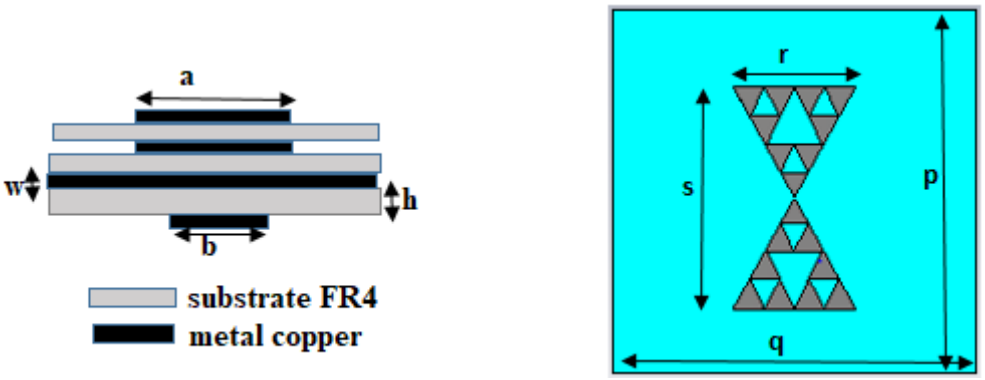

(a) (b)

Figure 3.8 (a) Front view of stacked antenna, (b) Top view of stacked antenna

The Figure 3.8 depicts top view of antenna. Both active and paracitic patches have same dimensions. The bow-tie patch has two triangles joined at the apex. Each triangle is subjected to two iterations, so as to make a sierpinski gasket individually of 2nd order.

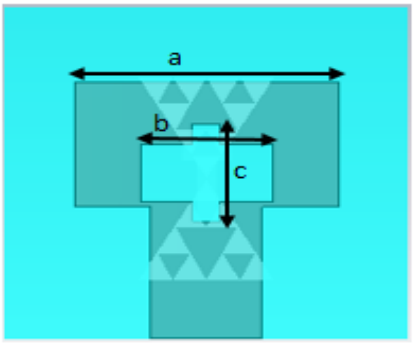

Figure 3.9 Partial ground of stacked structure with same patch above and below

Figure 3.9 shows the geometry of ground. The ground used is partial for proper impedance matching and to get a better bandwidth. With partial ground, the ground is defected with a plus shaped aperture slot. The optimization of the slot has been carried out to modify the desired results.

Table 3.2. Dimensions of stacked antenna

Parameters	**Dimensions(in mm)**
p	57.84
q	57.84
r	19.5
s	33.6
a	19.5
b	3
h	1.57
w	0.035
a	37.84
b	19
c	17

3.2.2 Simulation Results:

All the simulation results related to antenna designs were carried out using CST MWS version 2017. The simulation results in terms of impedance bandwidth, gain, radiation pattern and surface current distribution are presented in the next subsections.

3.2.2.1 Impedance Bandwidth:

The designed antenna resonates at lower frequencies 3.82 GHz, 4.1 GHz, 4.45 GHz and higher frequency 6.03 GHz. The bandwidth achieved is of 80 MHz (3.86-3.78 GHz), 90 MHz (4.14-4.05 GHz), 440 MHz (4.79-4.35) and 330 MHz (6.17-5.83GHz)**.** Figure 3.10 shows the simulated values of S_{11} having four bands.

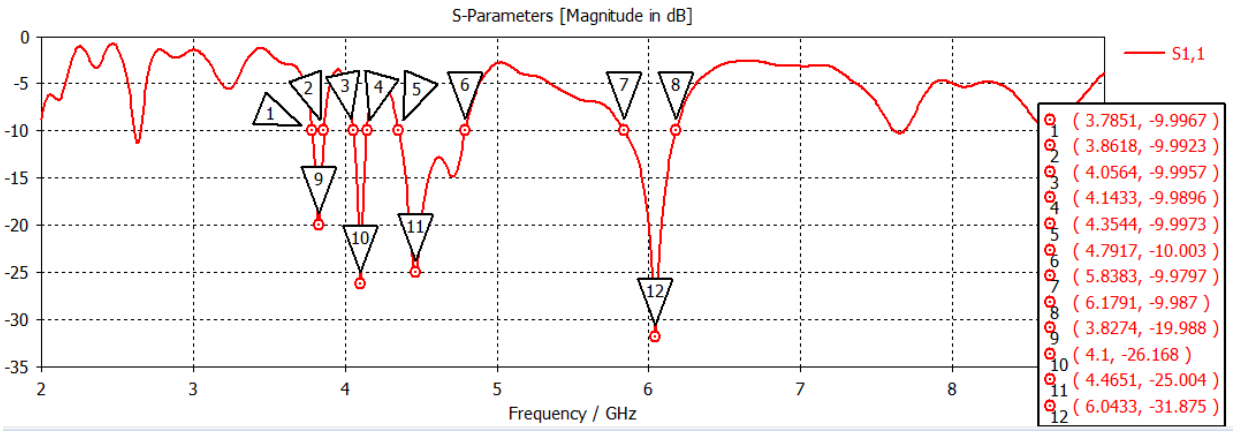

Figure 3.10 S_{11} parameter of stacked bow-tie antenna

3.2.2.2 Broadband Gain:

Figure 3.11 demonstrates frequency versus gain plot of presented antenna. However, overall broadband gain of the stacked sierpinski gasket fractal antenna is shown in this figure, which illustrates a peak gain of 5.40 dBi at 5.5 GHz and average gain of 4 dBi for the entire band of operation.

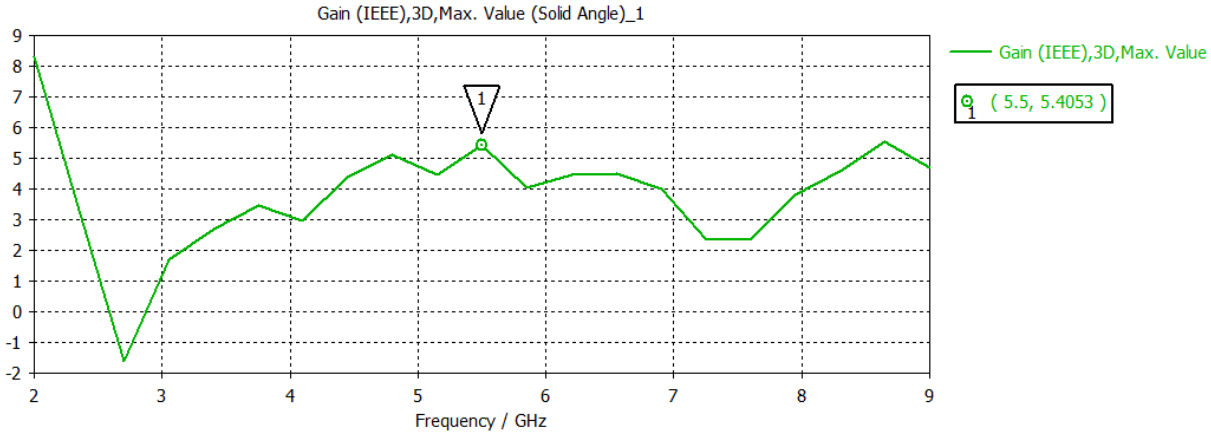

Figure 3.11 Overall broadband gain of the stacked bow-tie antenna

3.2.2.3 Radiation pattern:

Figure 3.12 demonstrates radiation pattern of antenna in terms of gain response at a resonant frequency of 4.45 GHz. Here, antenna shows a peak gain of 4.344 dBi, and polar plots of the radiation pattern is depicted in Figure 3.13.

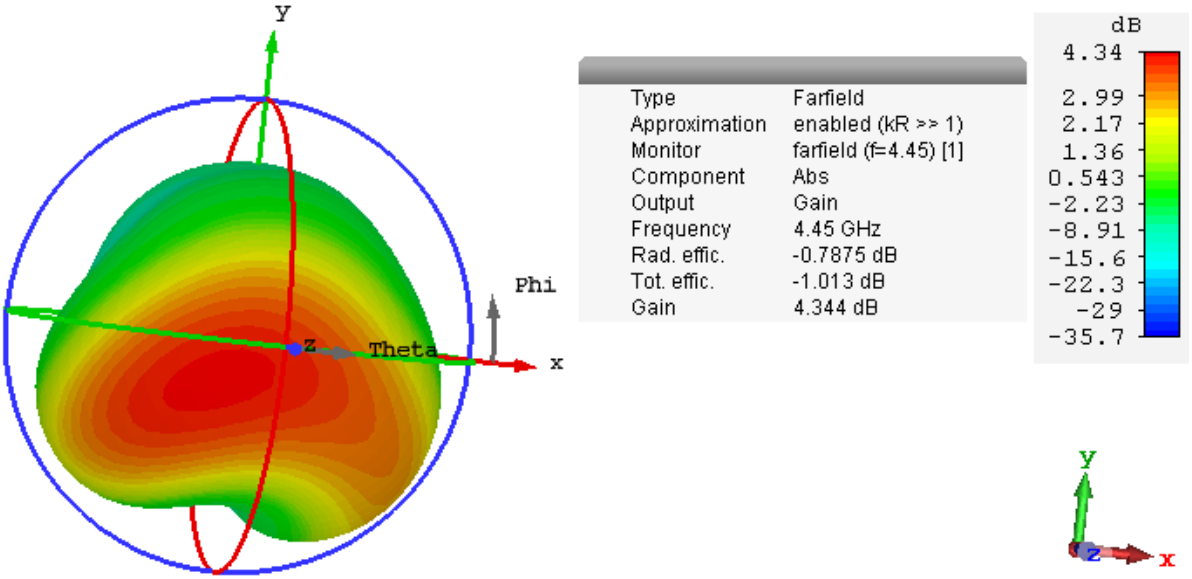

Figure 3.12 Radiation pattern of stacked bow-tie antenna

Figure 3.13 depicts that antenna has a major lobe along 7 degrees and a half power beamwidth of 69.8 degrees at 4.45 GHz.

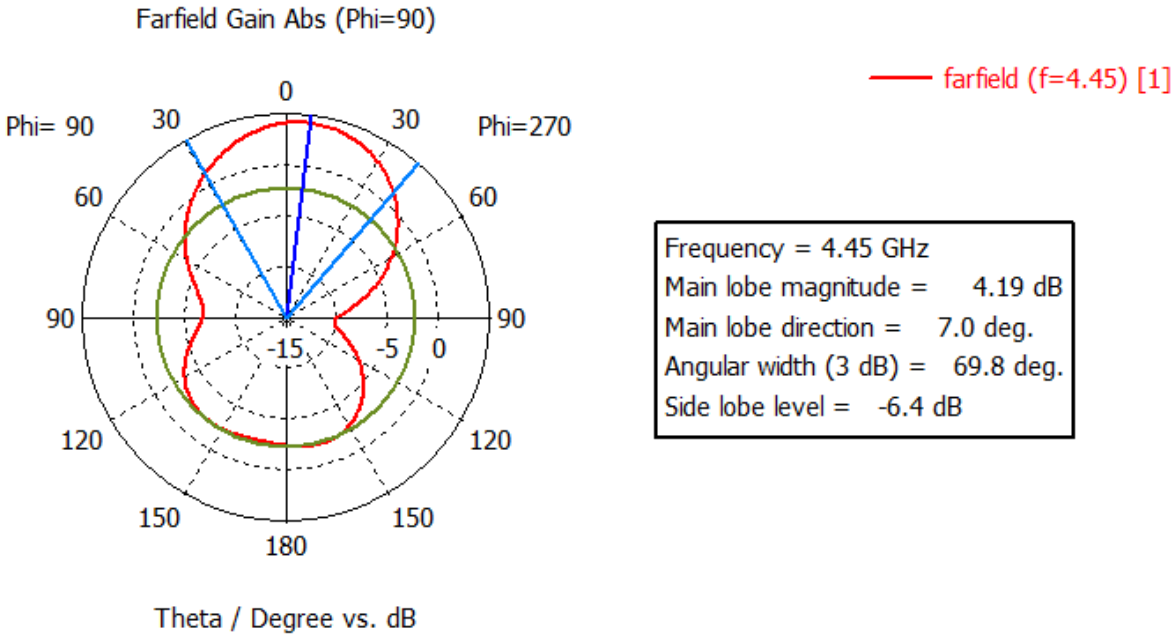

Figure 3.13 Polar plot of the stacked bow-tie antenna at 4.45 GHz

3.2.2.4 Surface current distribution:

Figure 3.14(a, b) shows surface current distribution of ground for resonant frequencies 4.45 GHz and 6.04 GHz, when antenna is excited using microstrip feedline in the software. For frequency of 6.04 GHz, the maximum current flows through the upper part of the plus slot and lower part of the partial ground. Figure 3.14(c, d) shows the magnitude of the current distribution of patch at frequencies 4.45 GHz as well as 6.04 GHz. The intensity of the current

is more at the upper triangle of the patch than that to at the apex. Figure 3.14(e, f) illustrates surface current distribution of strip line at frequencies 4.45 GHz and 6.04 GHz. The strip line have a stub, which really affects the magnitude of the current and has the maximum current density at the stub.

Hence, it can be concluded that upper triangle of the bow-tie patch, and upper part of the plus slot are responsible for resonating lower resonant frequency of 4.45 GHz, and feedline is responsible for resonating upper frequency of 6.04 GHz.

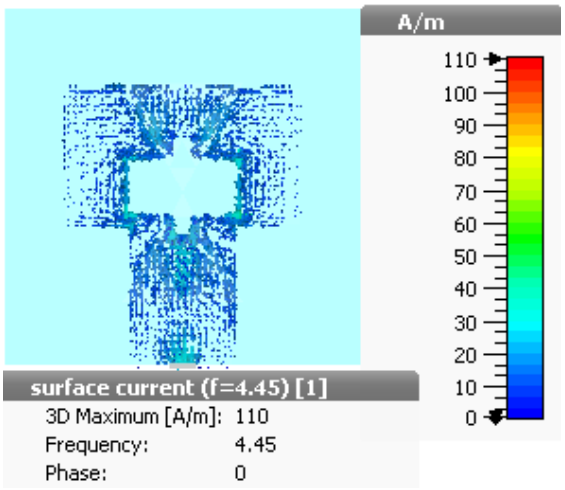

(a)

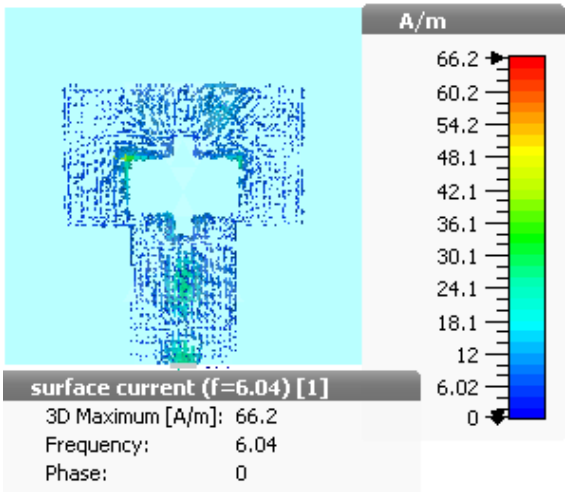

(b)

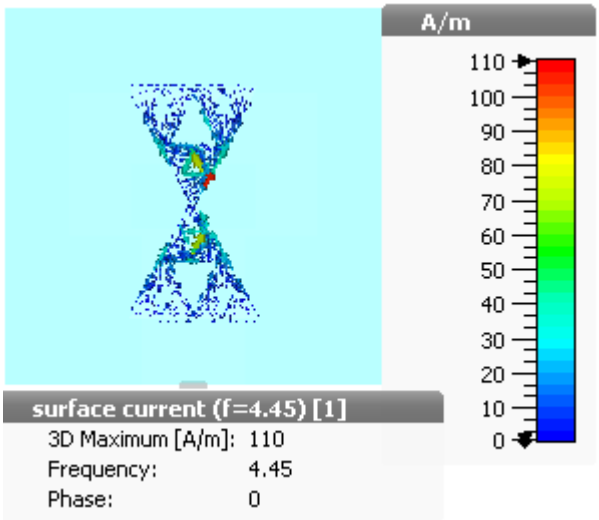

(c)

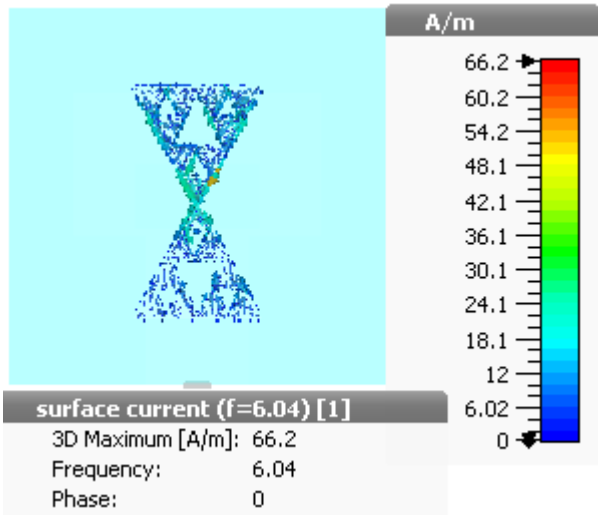

(d)

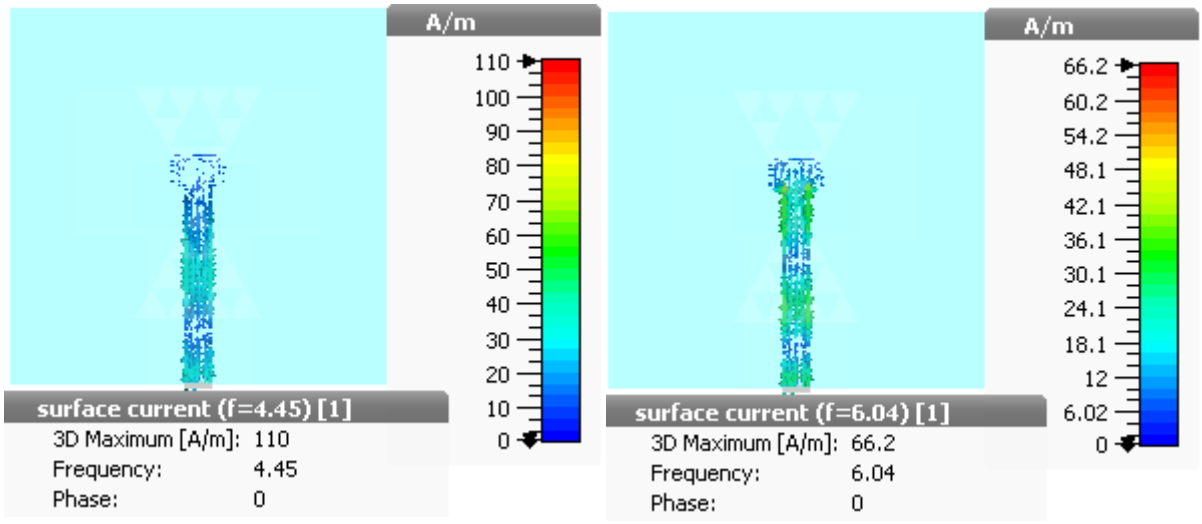

(e) (f)

Figure 3.14 Surface current distribution of presented antenna at resonating frequencies (a, c, e) 4.45 GHz (b, d, f) 6.04 GHz

3.2.3 Wireless Application Covered By Proposed Antenna:

The presented antenna exhibits bandwidth of 80 MHz (3.86-3.78 GHz), 90 MHz (4.14-4.05 GHz), 440 MHz (4.79-4.35) and 330 MHz (6.17-5.83GHz), which is used for short range Wi-Fi, wireless broadband and some cordless telephone. Also, this antenna is suitable for G band (3.95-5.85 GHz), E band (3.30-4.90 GHz).

3.3 STACKED STRUCTURE WITH A PARACITIC PATCH 3/4TH OF THE SIZE OF STANDARD PATCH BELOW:

The geometry presented in this section is same as stacked structure mentioned in above section. The variation is that the parasitic patch is made 3/4th of the size of standard patch below. Due to the scaling of the parasitic patch, the resonances get excited on higher frequency. The partial ground is same, but the plus slot has been optimized so as to get a good bandwidth.

3.3.1 Antenna Geometry:

Figure 3.15 shows the top view of partial ground of stacked geometry using a parasitic patch 3/4th of the size of standard patch below. The ground is partial with ‘T’ shape and having a plus slot in it. The optimization of the slot has been carried out to modify the desired results. The various antenna parameters of front and top view of antenna with their parametric values are discussed in Table 3.3.

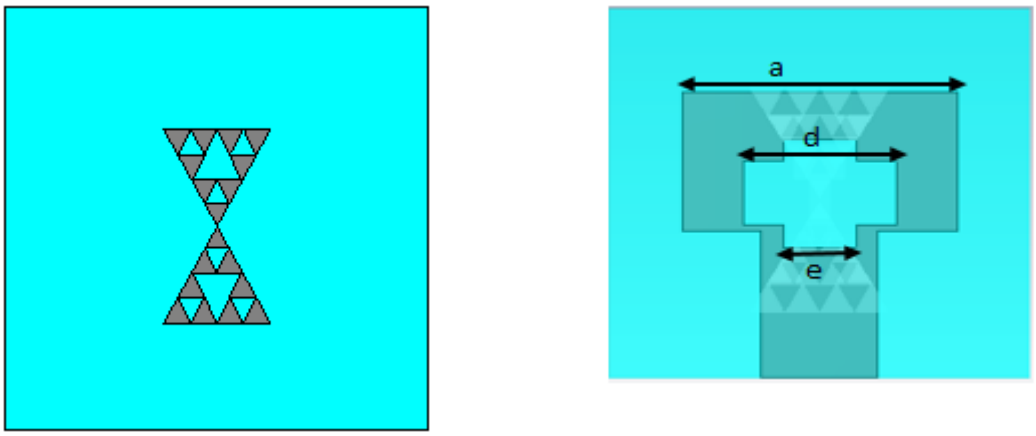

(a) (b)

Figure 3.15 (a) Top view of proposed antenna, (b) Partial ground using optimised plus slot of stacked structure with smaller patch above

Table 3.3 Dimensions of partial ground mentioned above

Parameters	**Dimensions(in mm)**
a	37.84
d	21
e	10

3.3.2 Simulation Results:

The antenna design discussed above is simulated by utilising CST microwave studio version 2017. Simulation results in terms of impedance bandwidth, current distribution and gain are presented in next subsections.

3.3.2.1 Impedance Bandwidth

The designed antenna resonates at lower frequencies 4.42 GHz, 4.93 GHz, and higher frequency 7.92 GHz. The bandwidth achieved is of 160 MHz (4.43-4.5 GHz), 1120 MHz (4.80-5.92 GHz), and 420 MHz (7.71-8.13 GHz)**.** Figure 3.16 shows the simulated values of S_{11} having three bands.

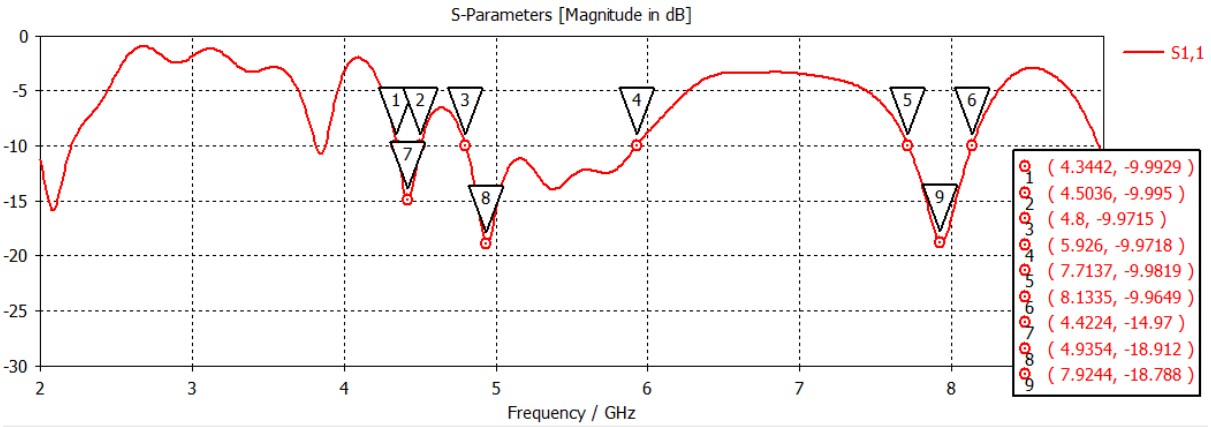

Figure 3.16 S_{11} parameter of presented antenna

3.3.2.2 Broadband Gain:

The overall broadband gain of stacked sierpinski gasket fractal antenna is shown in Figure 3.17 that shows a peak gain of 5.34 dBi at 4.6 GHz and average gain of 5 dBi overall entire band. A good gain antenna can be used for long range wireless applications.

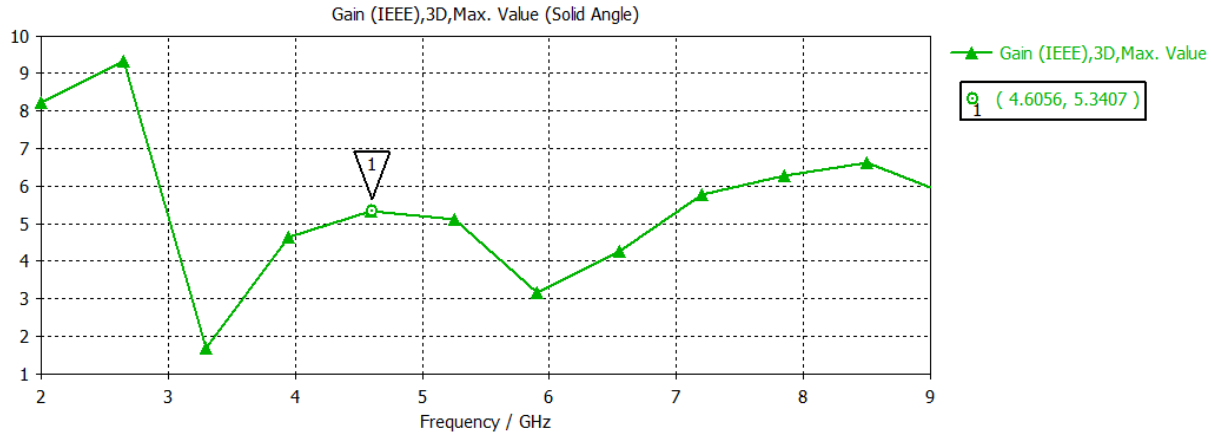

Figure 3.17 Overall broadband gain of the stacked antenna

3.3.2.3 Radiation pattern:

Figure 3.18 shows the 3D plot at the frequency 5.5 GHz that shows a peak gain of 5.16 dB approx. The radiation efficiency and total efficiency are also mentioned in the Figure 3.18, which shows polar plot of the stacked bow-tie antenna at 5.5 GHz frequency. Figure 3.19 shows that the antenna has a major lobe direction along 138 degree and half power beamwidth of 51.9 degrees.

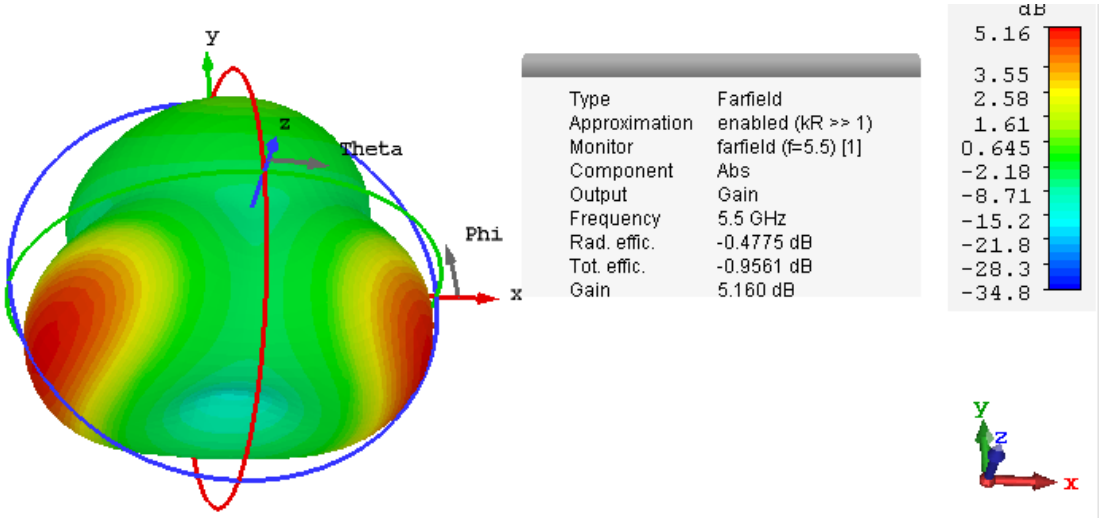

Figure 3.18 Radiation pattern of presented antenna at 5.5 GHz

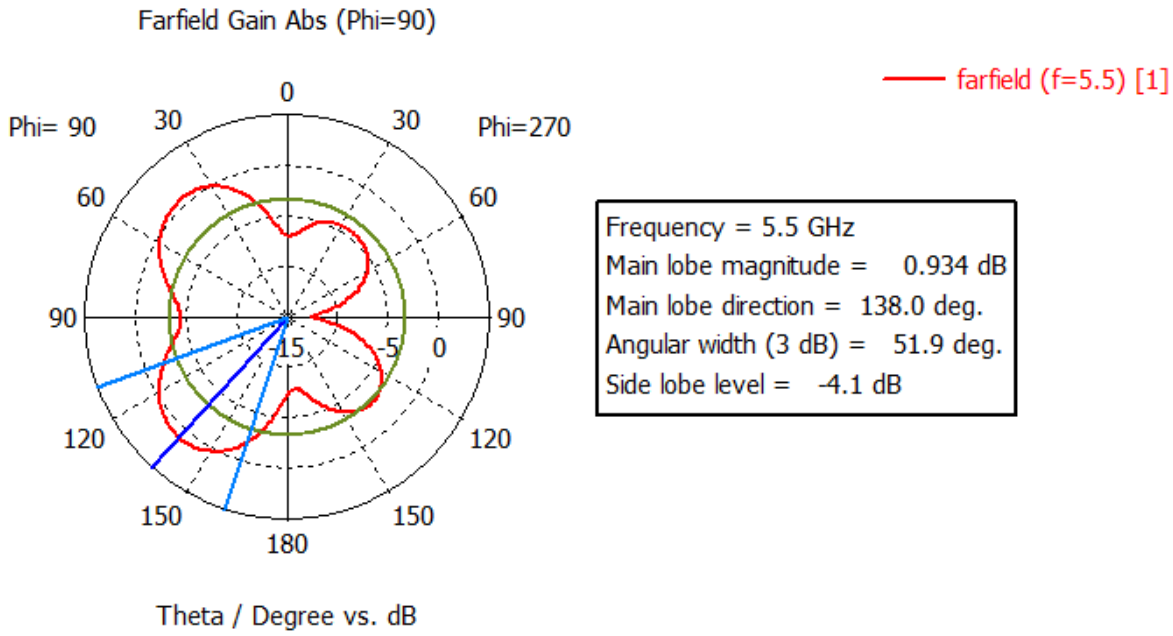

Figure 3.19 Polar plot of presented antenna at 5.5 GHz

3.3.2.4 Surface current distribution:

Figure 3.20(c, d) shows surface current distribution of ground for resonant frequencies 5.5 GHz and 4.93 GHz, when antenna is excited using microstrip feedline in the software. For frequency of 4.93 GHz, the maximum current flows through the lower part of the plus slot and lower part of the partial ground. Figure 3.20(a, b) indicates magnitude of current distribution of patch at frequencies 5.5 GHz and 4.93 GHz. However, intensity of the current is more at the upper triangle of the patch than that to at the apex. Figure 3.20(e, f) depicts surface current distribution of strip line at frequencies 5.5 GHz and 4.93 GHz. The strip line have a stub, which really affects the magnitude of the current, and has the maximum current density at the stub.

Hence, it can be concluded that upper triangle of the bow-tie patch and upper part of the plus slot are responsible for resonating lower resonant frequency of 4.93 GHz; and feedline is responsible for resonating upper frequency of 5.5 GHz.

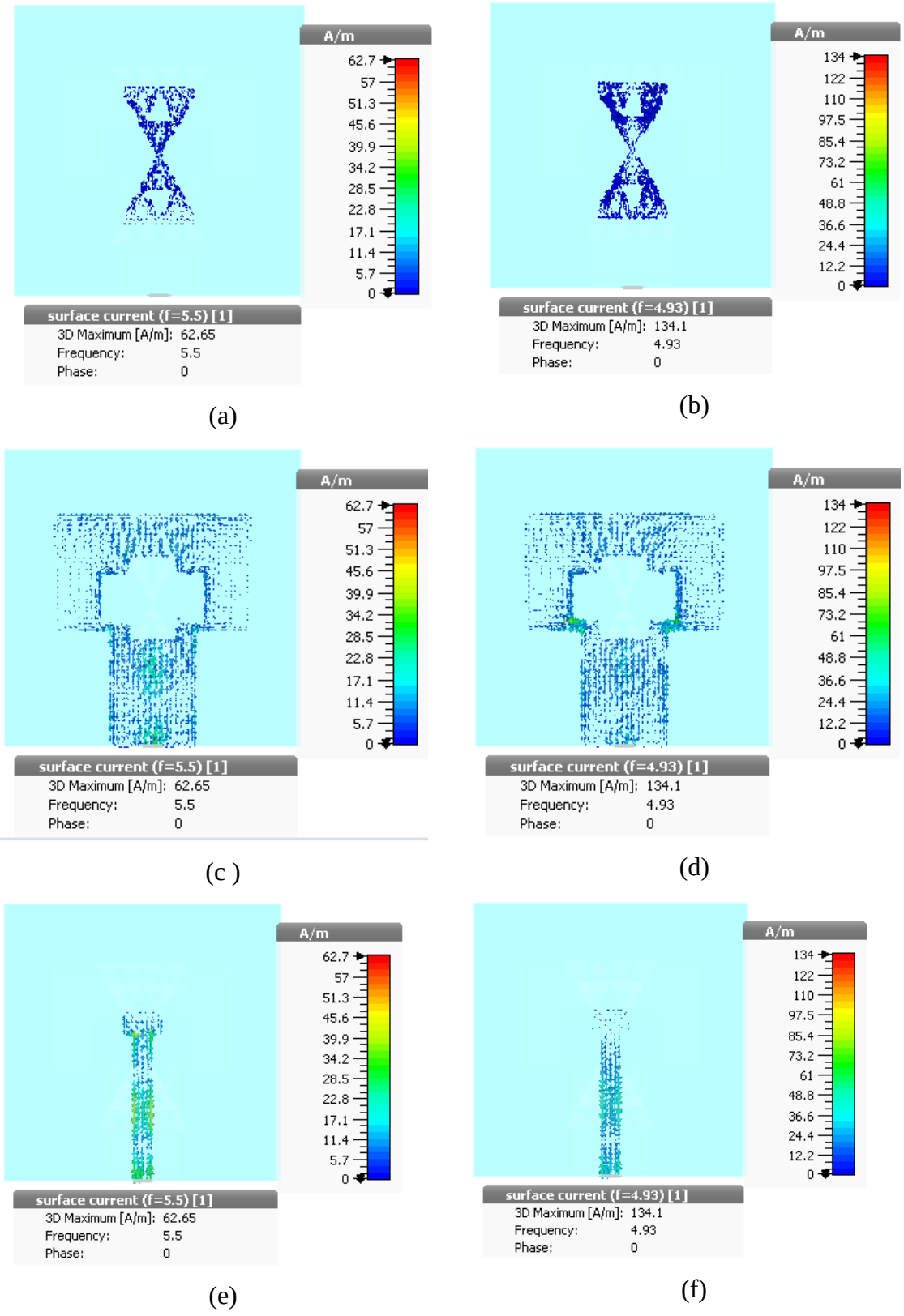

Figure 3.20 Surface current distribution of presented antenna at resonating frequencies (a, c, e) 5.5 GHz (b, d, f) 4.93 GHz

3.3.3 Wireless Application Covered By Proposed Antenna:

The presented antenna exhibits BW of 160 MHz (4.43-4.5 GHz), 1120 MHz (4.80-5.92 GHz), and 420 MHz (7.71-8.13 GHz), which is used for short range Wi-Fi, wireless broadband and some cordless telephone. Also the antenna is suitable for the G band (3.95-5.85 GHz), F band (4.90-7.05 GHz) and C band (5.85-8.20 GHz) wireless applications.

3.4 STACKED STRUCTURE WITH A ACTIVE PATCH 3/4TH OF THE SIZE OF STANDARD PATCH ABOVE:

In this geometry, the active patch is 25% shorter as compared to the size of standard parasitic patch. Due to this higher frequency, resonances get excited. And a bandwidth of 1250 MHz is achieved. Due to the scaling of the active patch, the resonances get excited on lower frequency. The partial ground is same, but the plus slot has been optimized so as to get good bandwidth results.

3.4.1 Antenna Geometry:

The antenna geometry is same as in previous case (refer to Figure 3.15(a)) but now the driven patch is 25% smaller than standard size of the stacked patch antenna.

Figure 3.21 depicts top perspective of partial ground with a stacked geometry. Here, the driven patch is 3/4th of the size of standard patch above. The ground is partial with 'T' shape and having a plus slot in it. The optimization of the slot has been carried out to modify the desired results. The various antenna parameters of front and top view of antenna with their parametric values are discussed in Table 3.4.

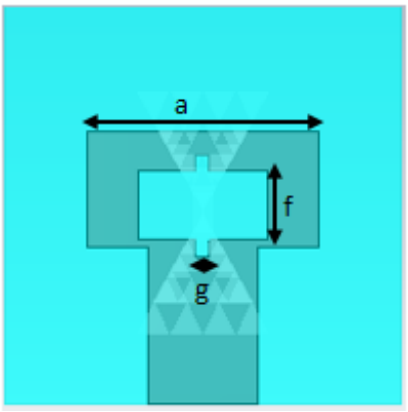

Figure 3.21 Partial ground with optimised plus slot of stacked structure with smaller patch below

Table 3.4 Dimensions of partial ground given above

Parameters	Dimension(in mm)
a	37.84
f	10
g	2

3.4.2 Simulation Results:

All the simulation results related to antenna designs were carried out using CST MWS version 2017. Simulation outcomes in terms of impedance BW, gain, radiation pattern as well as surface current distribution are presented in next subsections.

3.4.2.1 Impedance Bandwidth:

The designed antenna resonates at lower frequencies 5.24 GHz and higher frequency 7.38 GHz, 8.07 GHz. The BW achieved is of 190 MHz (5.15-5.34 GHz) and 1250 MHz (7.10-8.35 GHz). Figure 3.22 shows the simulated values of S_{11} having two bands.

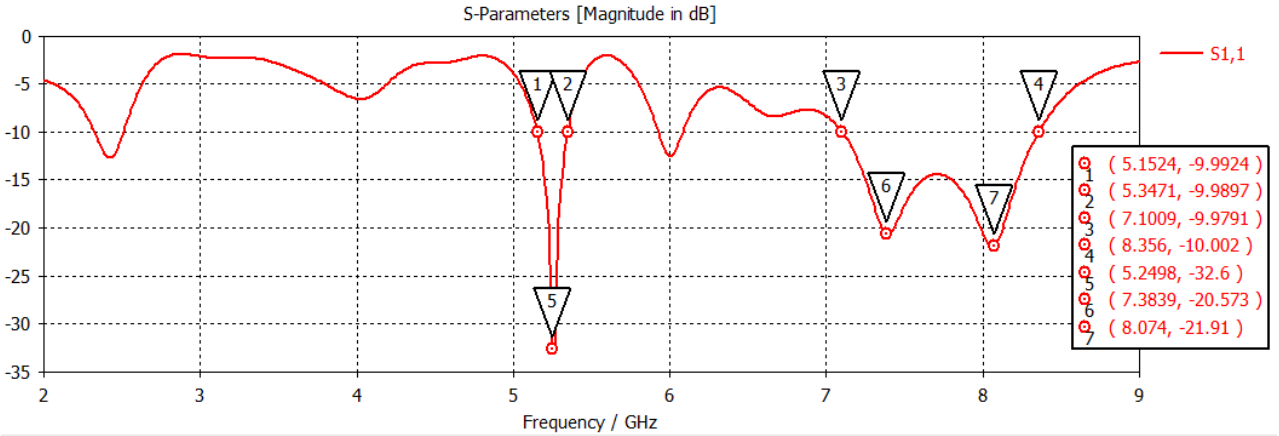

Figure 3.22 S_{11} parameter of the proposed antenna

3.4.2.2 Broadband Gain:

The overall broadband gain of the stacked sierpinski gasket fractal antenna has been demonstrated in Figure 3.23 that shows a peak gain of 4.199 dBi at 7.83 GHz and average gain of 4 dBi for the entire band. A good gain antenna can be used for long range wireless applications.

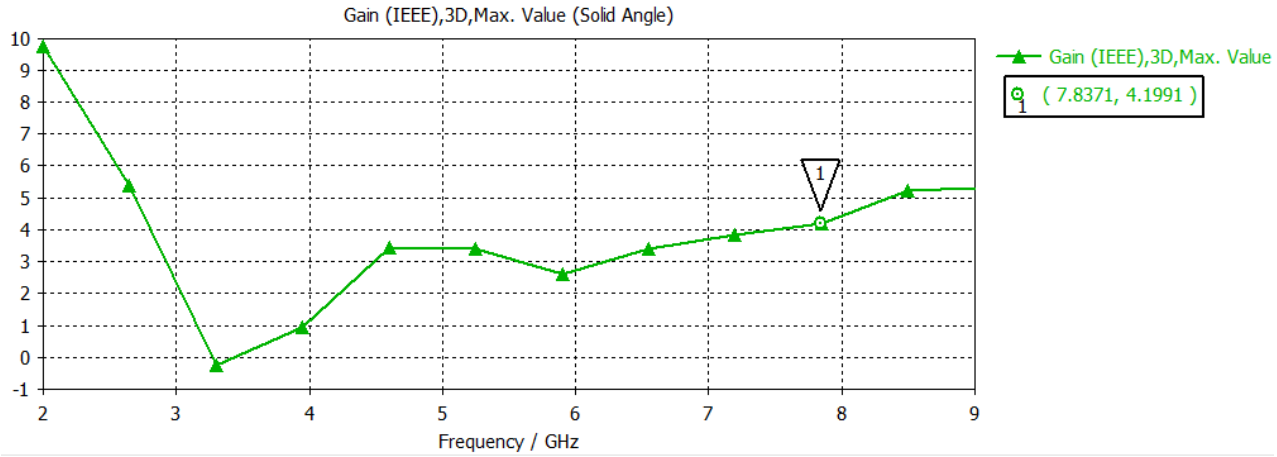

Figure 3.23 Overall broadband gain of the proposed antenna

3.4.2.3 Radiation pattern:

Figure 3.24 shows the 3D plot at the frequency 8.05 GHz that shows a peak gain of 4.59 dB approx. The radiation efficiency and total efficiency are also mentioned in the Figure 3.24. Figure 3.24 shows polar plot of the stacked bow-tie antenna at 8.05 GHz frequency. Figure 3.25 shows that the antenna has a major lobe direction along 160 degree and half power beamwidth of 111.1 degrees.

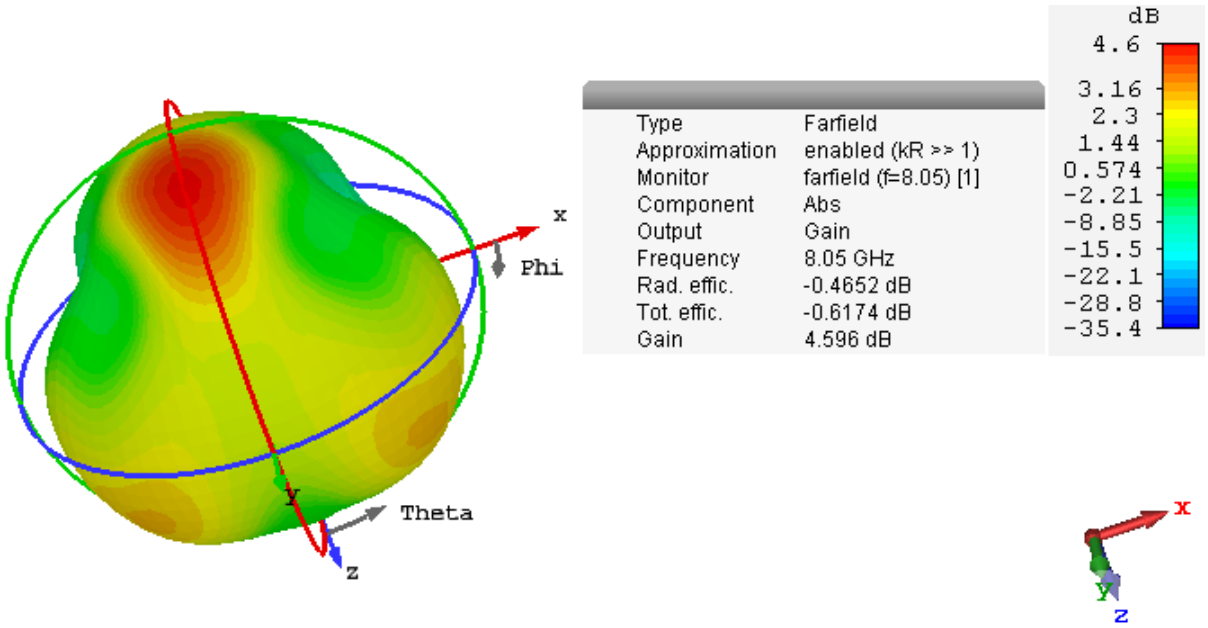

Figure 3.24 Radiation pattern of presented antenna

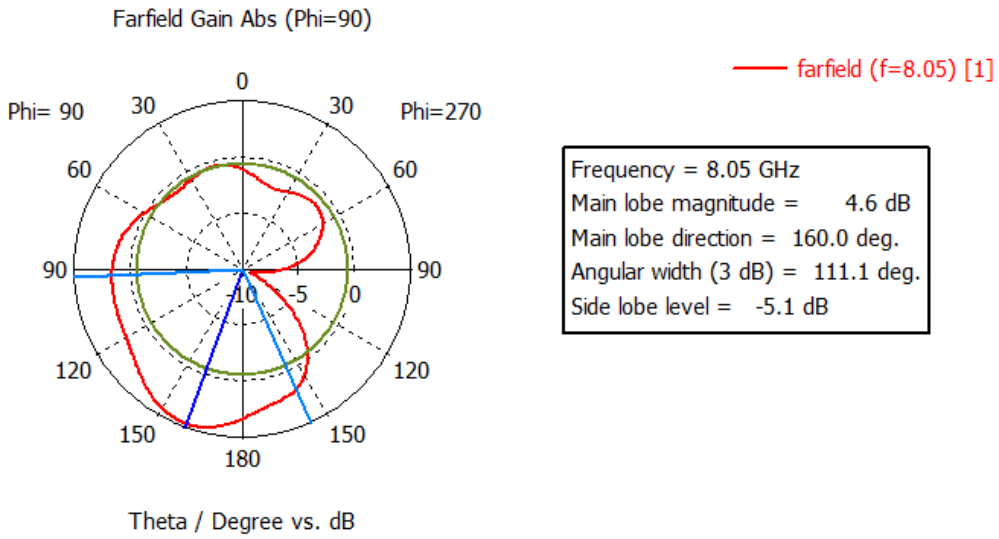

Figure 3.25 Polar plots of presented antenna at frequency 8.05 GHz

3.4.2.4 Surface current distribution:

Figure 3.26(a, b) depicts surface current distribution of the ground for resonant frequencies 5.24 GHz and 7.38 GHz, when antenna is excited using microstrip feedline in the CST software. For frequency of 7.38 GHz, the maximum current flows through the lower part of the plus slot and lower part of the partial ground. Figure 3.26(c, d) show the magnitude of the current distribution of patch at frequencies 5.24 GHz and 7.38 GHz. The intensity of the current is more at the upper triangle of the patch than that to at the apex. Figure 3.26(e, f) depicts surface current distribution of strip line at frequencies 5.24 GHz and 7.38 GHz. The strip line has a stub, which really affects the magnitude of the current, and has the maximum current density at the stub.

Hence, it can be concluded that upper triangle of the bow-tie patch, and lower part of the plus slot are responsible for resonating lower resonant frequency of 5.24 GHz, and feedline is responsible for resonating upper frequency of 7.38 GHz.

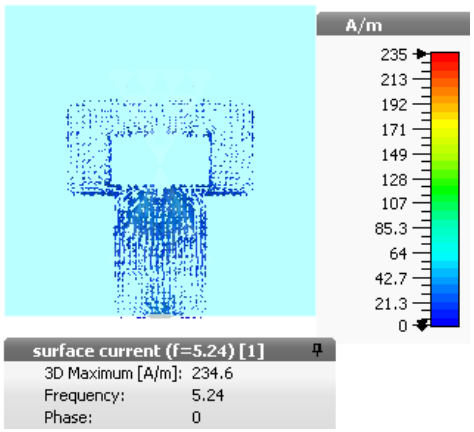

(a)

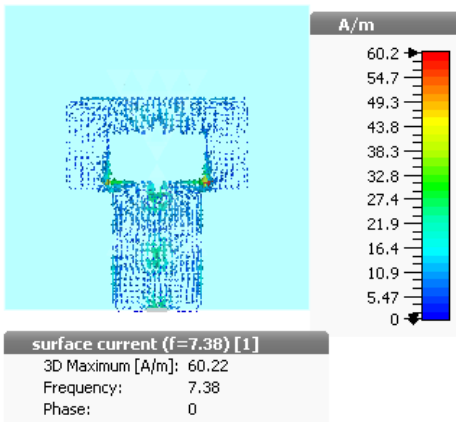

(b)

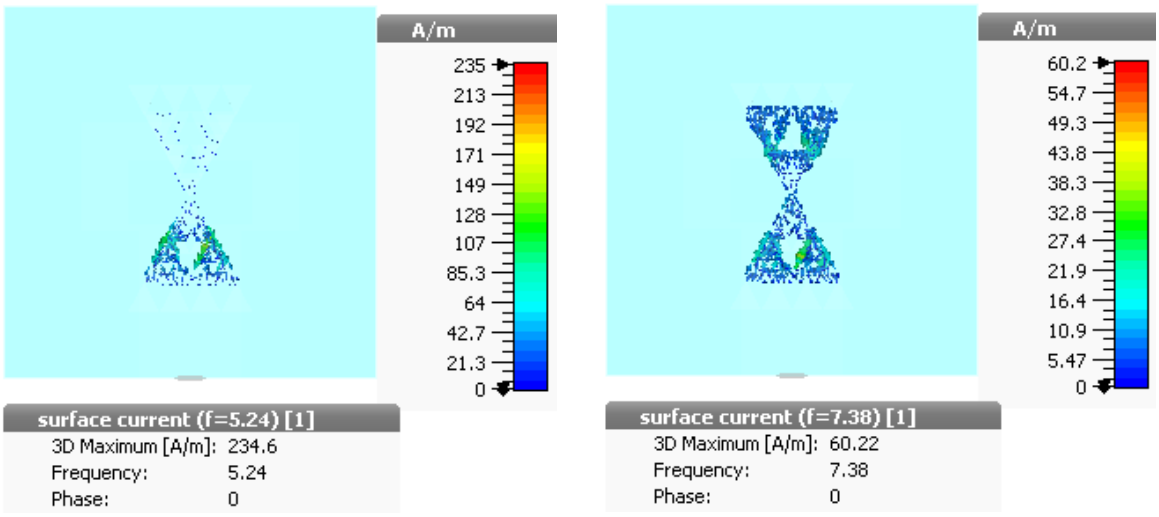

(c) (d)

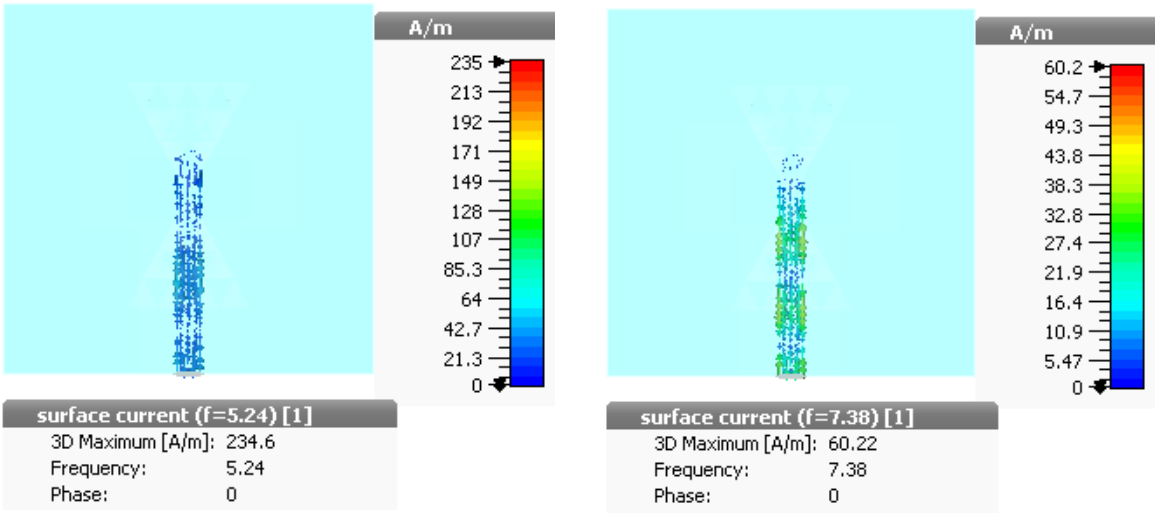

(e) (f)

Figure 3.26 Surface current distribution of presented antenna at resonating frequencies (a, c, e) 5.24 GHz (b, d, f) 7.38 GHz

3.4.3 Wireless Application Covered By Proposed Antenna:

The presented antenna exhibits BW of 190 MHz (5.15-5.34 GHz) and 1250 MHz (7.10-8.35 GHz), which is used for short range Wi-Fi, wireless broadband and some cordless telephone. Also the antenna is suitable for the G band(3.95-5.85 GHz), F band (4.90-7.05 GHz) , C band (5.85-8.20 GHz) and H band (7.05-10.10 GHz).

Table 3.5 shows the comparitive analysis of all three types of stacked geometries in terms of resonant frequencies, impedance bandwidth.

Table 3.5 Comparison of three stacked geomerties mentioned in above sections

Geometries	**Resonances**	**Impedance BW**	**Peak Gain**	**Applications**
Geometry 1	3.82 GHz, 4.1 GHz, 4.45 GHz, 6.03 GHz.	80 MHz, 90 MHz, 440 MHz, 330 MHz resp. at the three bands.	5.4 dBi	Short range Wi-Fi, wireless broadband, some cordless telephone, G band, E band.
Geometry 2	4.42 GHz, 4.93 GHz, 7.92 GHz.	160 MHz, 1120 MHz, 420 MHz.	5.34 dBi	G band, F band, C band.
Geometry 3	5.24 GHz, 7.38 GHz, 8.07 GHz	190 MHz, 1250 MHz	4.19 dBi	G band, F band, C band, H band.

From the comparison analysis of all the three stacked sierpinski gasket fractal geometries, the best one among three of them is geometry 1 of same dimensions of active and parasitic patches. This geometry shows more resonances of good bandwidth as compared to other two geometries. The highest gain among three geometries is 5.4 dBi, which is of geometry 1. So, the best geometry among the three is geometry 1. And it concludes that stacked MSA with identical active and parasitic patch is most efficient.

3.5 CONCLUSION:

The chapter presents comparative analysis of four aperture coupled fractal microstrip antenna geometries. This has been observed that unstacked geometry proposed above shows two resonances at 4.317 GHz and 8.28 GHz with a bandwidth of 380 MHz and 270 MHz respectively. A stacked structure with same dimension on the above and below patch shows four resonances at 3.82 GHz, 4.1 GHz, 4.46 GHz and 6.04 GHz with BW of 440 MHz, 90 MHz, 80 MHz and 330 MHz respectively because of partial ground. Stacked structure with patch $3/4^{th}$ of the size of standard patch below covers resonances of 3.846 GHz, 4.418 GHz, 4.937 GHz and 7.928 GHz with bandwidth of 1120 MHz, 160 MHz and 420 MHz respectively. Fourth structure with patch below $3/4^{th}$ of the size of standard patch above shows resonances at 5.25 GHz, 6.00 GHz, 7.394 GHz and 8.057 GHz with BW of 190 MHz, 160 MHz and 1250 MHz. It is also seen that a stacked structure with same sized antenna on both the driven and parasitic layers shows highest impedance bandwidth, gain and directional characteristics. The unstacked structure is suitable for WLAN and ITU satellite communication band. The stacked structures covers E, G and C bands, which are used for short range Wi-Fi, wireless broadband and some cordless telephone.

CHAPTER-4

DESIGN AND SIMULATION OF AN UNSTACKED AND STACKED DIAMOND SHAPED SIERPINSKI GASKET FRACTAL MICROSTRIP ANTENNA

This chapter describes the design as well as simulation of a diamond shaped sierpinski gasket fractal antenna with three level of iterations. An unstacked diamond structure is presented first. In order to improve its output characteristics, stacking of this antenna with another diamond shaped parasitic patch is done. Based upon the comparative analysis done in previous chapter; the parasitic patch is chosen to be of same dimension as that of driven one. Next subsection presents the antenna design and performance analysis.

4.1 UNSTACKED DIAMOND SIERPINSKI GASKET FRACTAL ANTENNA:

This section presents the designing and simulation of the unstacked diamond sierpinski gasket fractal microstrip antenna using defected ground configuration. In afore mentioned sections, sierpinski gasket showed a good bandwidth, and this is the reason to continue researching on it with different shape i.e., rhombus. The type of antenna preferred here is strip line instead of aperture coupled. The design parameters and simulation results are discussed in section below.

4.1.1 Antenna Design and Specifications:

The proposed antenna in this section is of microstrip structure i.e., the feedline is straight attached to patch. Here, patch is of rhombus shape and is optimised till three level of iterations.

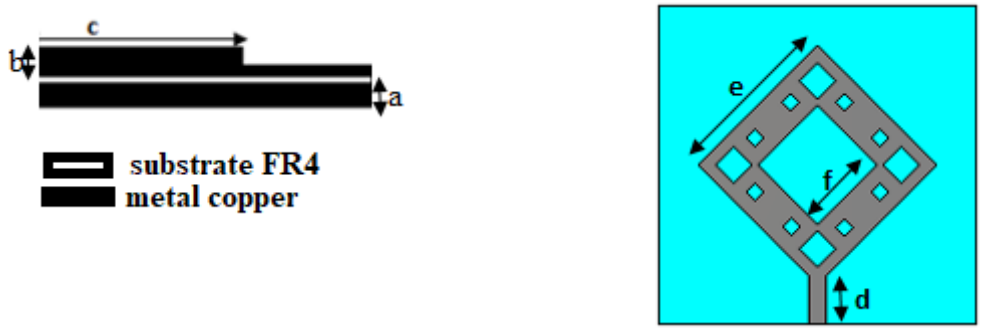

(a) (b)

Figure 4.1 (a) Front perspective of unstacked stripline antenna,
(b) Top perspective of the antenna i.e., patch with a feedline

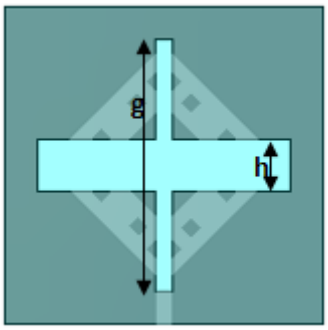

Figure 4.2 Illustrates top view of defected ground of unstacked sierpinski diamond fractal antenna

The various antenna parameters of front and top view of antenna with their parametric values are discussed below:

Table 4.1 Dimensions of unstacked antenna

Parameters	**Dimension(in mm)**
Height of ground (a)	0.035
Height of patch(b)	0.035
c	32.85
d	4.85
e	20
f	10
g	30
h	6

4.1.2 Simulation Results and Discussions:

In this section, a sierpinski gasket fractal aperture coupled antenna is developed as well as simulated by utilizing CST MWS V'17. The simulation outcomes are analysed in terms of return loss, BW, gain as well as current distribution

4.1.2.1 Impedance bandwidth:

The designed antenna resonates at lower frequencies 5.45 GHz, and higher frequency 6.22 GHz, 7.81 GHz. The bandwidth achieved is of 90 MHz (5.42-5.51 GHz), 370 MHz (6.04-6.41 GHz), and 390 MHz (8.00-7.61GHz)**.** Figure 4.3 shows the simulated values of S_{11} having three bands.

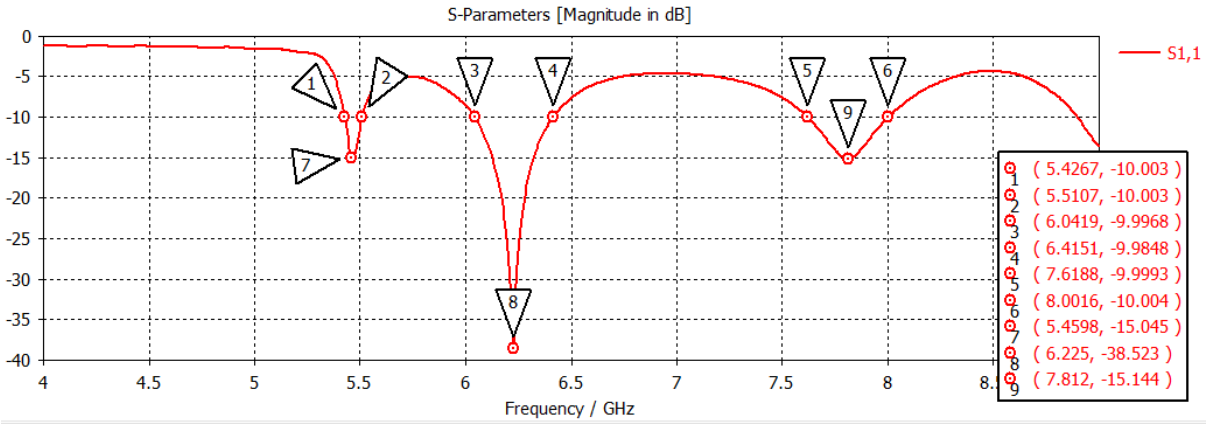

Figure 4.3 Simulated S_{11} (dB) plot of unstacked diamond antenna

4.1.2.2 Broadband Gain:

The overall broadband gain of the diamond sierpinski gasket is shown in Figure 4.4 that shows a peak gain of 7.33 dBi at 6.24 GHz and average gain of 6 dBi for the entire band. A good gain antenna can be used for long range wireless applications.

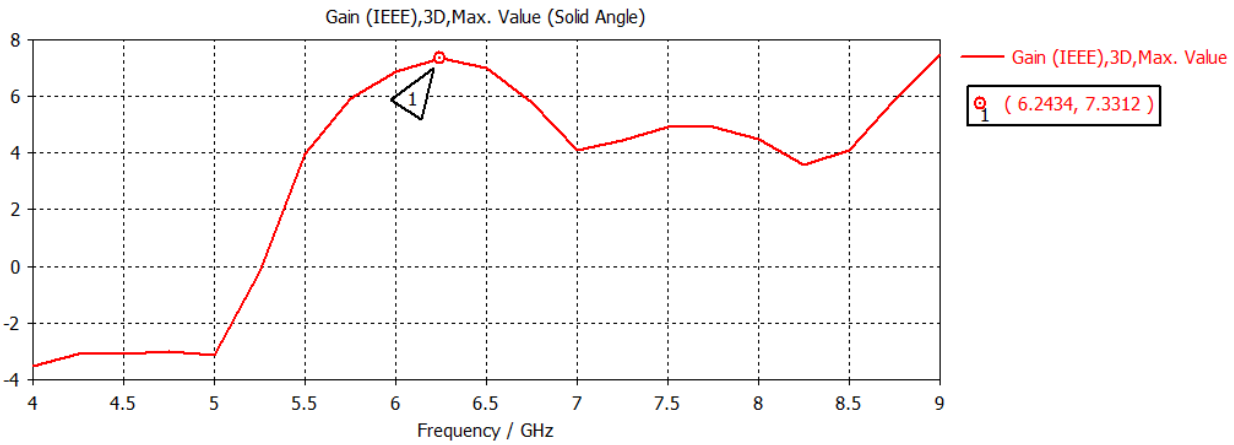

Figure 4.4 Simulated broadband gain of the proposed antenna

4.1.2.3 Radiation Pattern:

Figure 4.5 demonstrates radiation pattern of antenna in terms of gain at a resonant frequency of 6.22 GHz. Here, antenna shows a peak gain of 7.32 dBi, and the polar plots of the radiation pattern are shown in Figure 4.6. The antenna has a major lobe along 176 degrees and a half power beamwidth of 68.1 degrees

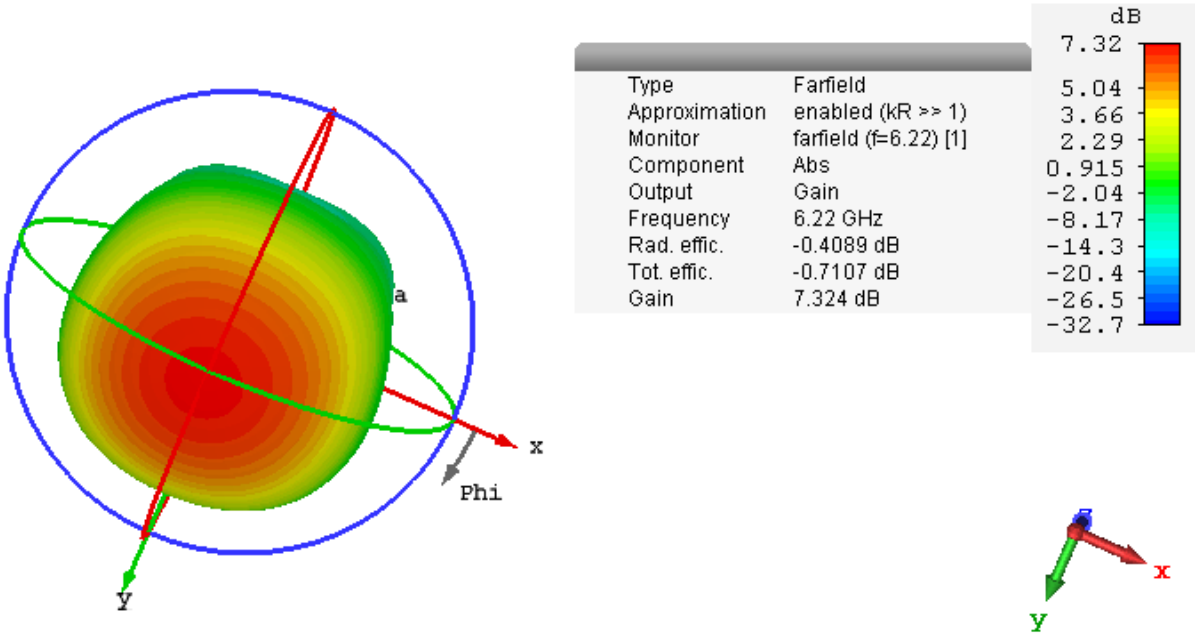

Figure 4.5 Radiation pattern of the proposed antenna

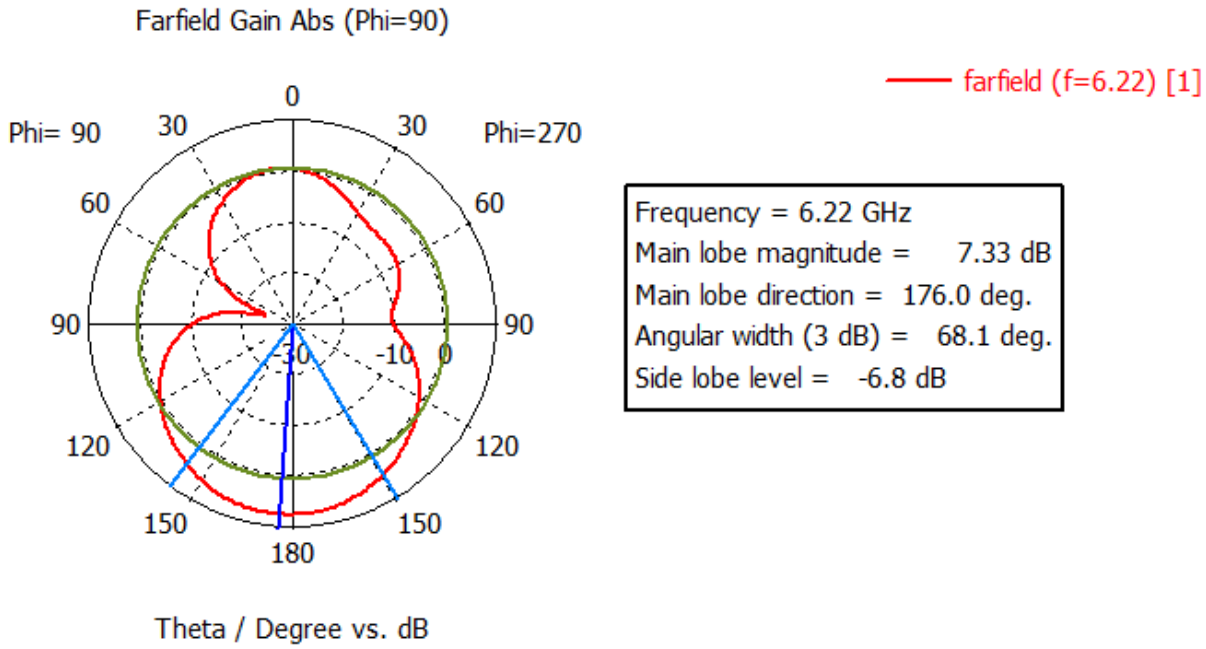

Figure 4.6 Polar gain plot at 6.22 GHz

4.1.2.4 Surface Current Distribution:

Figure 4.7(a-f) show current distribution on various layers of antenna for resonant frequencies of 6.22 GHz and 7.81 GHz, when antenna is energized utilizing an aperture coupled feeding in software. A comparative study of surface current on various layers of antenna leads to the conclusion that top patch is responsible for exciting 6.22 GHz frequency.

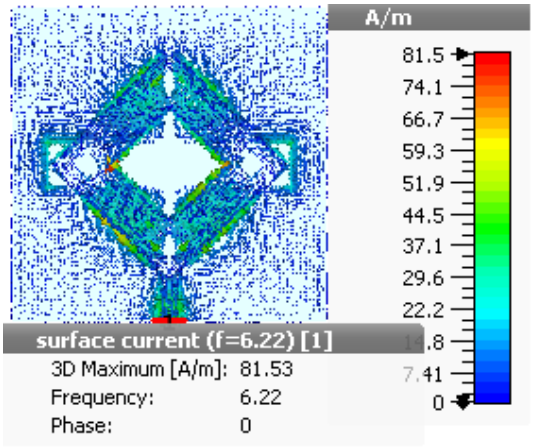

(a)

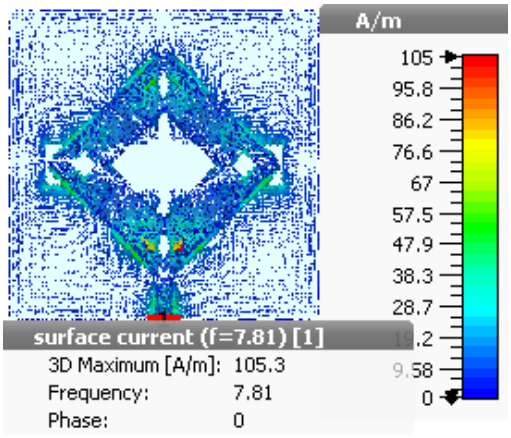

(b)

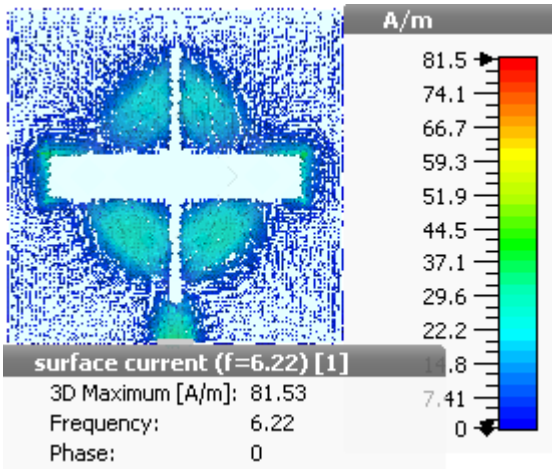

(c)

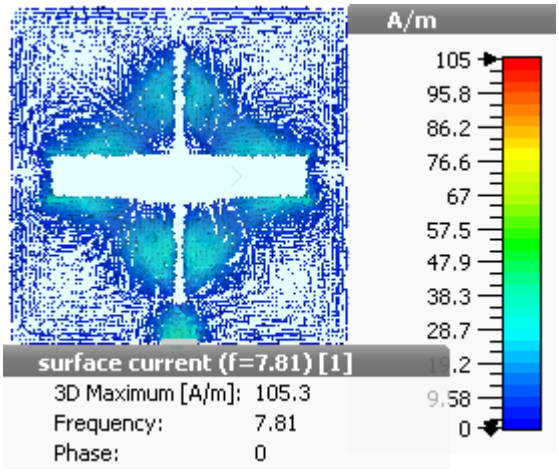

(d)

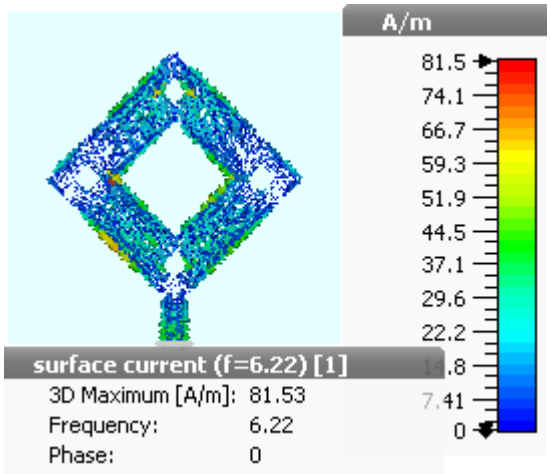

(e)

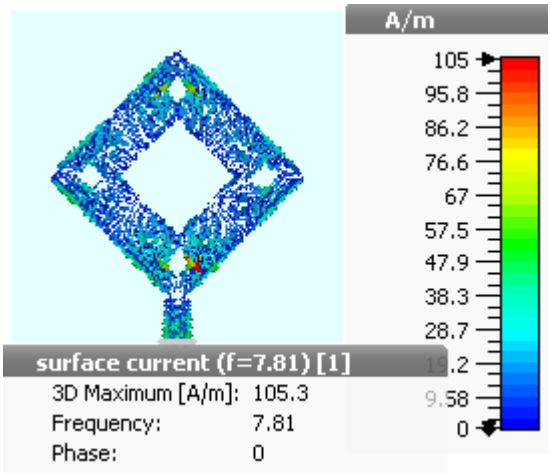

(f)

Figure 4.7 Surface current distribution of presented antenna at resonating frequencies (a, c, e) 6.22 GHz (b, d, f) 7.81 GHz

4.1.3 Wireless Application Covered By Proposed Antenna:

The presented antenna exhibits BW of 90 MHz (5.42-5.51 GHz), 370MHz (6.04-6.41 GHz), and 390 MHz (8.00-7.61GHz), which is used for some weather radar system, short range Wi-Fi, wireless broadband and some cordless telephone. Also the antenna is suitable for the G band (3.95-5.85 GHz), F band (4.90-7.05 GHz) and C band (5.85-8.20 GHz).

In order to observe the effect of stacking, a same sized patch is drawn over the driven one. Next section presents the design and preformance evaluation of a stacked diamond shaped antenna with same size driven and parasitic patch.

4.2 STACKED DIAMOND SIERPINSKI GASKET FRACTAL ANTENNA:

The design as well as performance evaluation of the sierpinski Gasket Diamond stacked fractal antenna for multiple band application are presented. Fractal antenna shapes are applied to a conventional diamond shaped microstrip patch antenna with three level of iterations to achieve the multiband performance. The use of partial ground has been illustrated to achieve better results. The proposed stacked sierpinski gasket diamond shaped fractal antenna shows impedance bandwidth of 1.29 GHz for the frequency bands from 5.46 GHz to 6.75 GHz. A peak gain of 6.833 dBi at 5.5 GHz allows the antenna to be suitable for WLAN and various wireless communication applications.

4.2.1 Antenna Geometry:

Figure 4.8 shows that the geometry of the designed stacked antenna has three layers. The bottom most layer is ground, which is of 0.0035 mm height, and its material is perfect electric conductor. The ground is a partial ground with a '+' shaped slot cut out from it. The middle layer is FR4 substrate of height 1.57 mm, and on top of it a patch of diamond shape is designed with micro stripline feed. The shape of the patch is rhombus i.e., all the sides are congruent to each other. Sierpinski gasket fractal defects are cut out from the patch upto 3rd iteration to achieve better results in terms of multiband performance. The top most layer is of FR4 substrate, and this has an identical patch (as the driven) printed on it, this is a parasitic patch, and it results in modification of impedance bandwidth of antenna. Here, dimension of both the active and parasitic patch are same. Table 4.2 mentions design parameters of antenna.

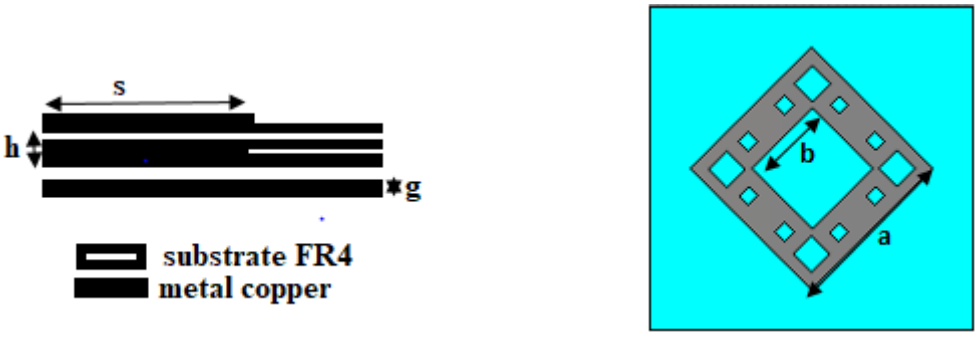

(a) (b)

Figure 4.8 (a) Front perspective of antenna, (b) Top perspective of antenna

The topmost view of the antenna is shown below with the dimension of the diamond (rhombus) shaped patch. The side of the outer most rhombus is 20 mm, and a small rhombus scaled half of the bigger rhombus of side 10mm is cut from the bigger rhombus. Four smaller rhombus are cut, which is 70% scaled version of 10mm rhombus. Another six small rhombuses are cut to get fractal shape upto 3rd iteration.

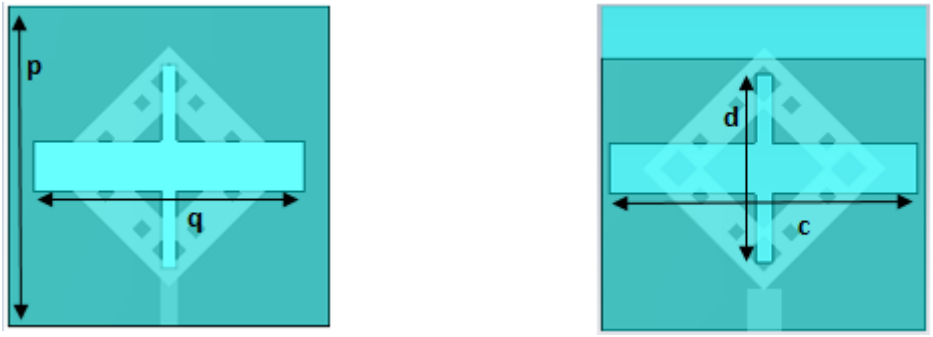

(a)

(b)

Figure 4.9 (a) Top view of normal ground, (b) Top view of partial ground

Firstly, the defected ground of height 0.035 mm was made with a plus like slot in it. The width of the horizontal slot was more than that of the vertical slot. As the dimensions are fixed by optimising both the vertical and horizontal slots. The top view of the normal ground is depicted in Figure 4.9 (a).

Figure 4.9 (b) illustrates top view of partial ground, which is designed to enhanced BW of antenna. The x-axis of the partial ground is kept unvaried, but y-axis of the ground is decreased. Here, height of the ground have been optimised to 31.7 mm from 37.7 mm. The simulated

results are shown in next section, which shows improvement in bandwidth by using partial ground. Table 4.2 mentions the designed parameter of the antenna design.

Table 4.2 Dimensions of stacked antenna

Parameters	Dimensions(in mm)
Side of rhombus(s)	20
Width of stripline(h)	2
Height of ground(g)	0.035
a	20
b	10
p	37.7
q	32
c	36
d	22

4.2.2. Simulation Results:

The presented stacked fractal antenna was development as well as simulated using CST MWS V2017. Simulations were carried out using perfect boundary conditions.

4.2.2.1 S Parameter Bandwidth:

Figure 4.10 shows the simulated value of S_{11} with partial ground. The result has multiple resonant band from 4.95 GHz to 5.04 GHz, 5.40 GHz to 6.72 GHz and 6.95 GHZ to 7.25 GHz. This allows the antenna to be suitable for G, F and C bands wireless applications.

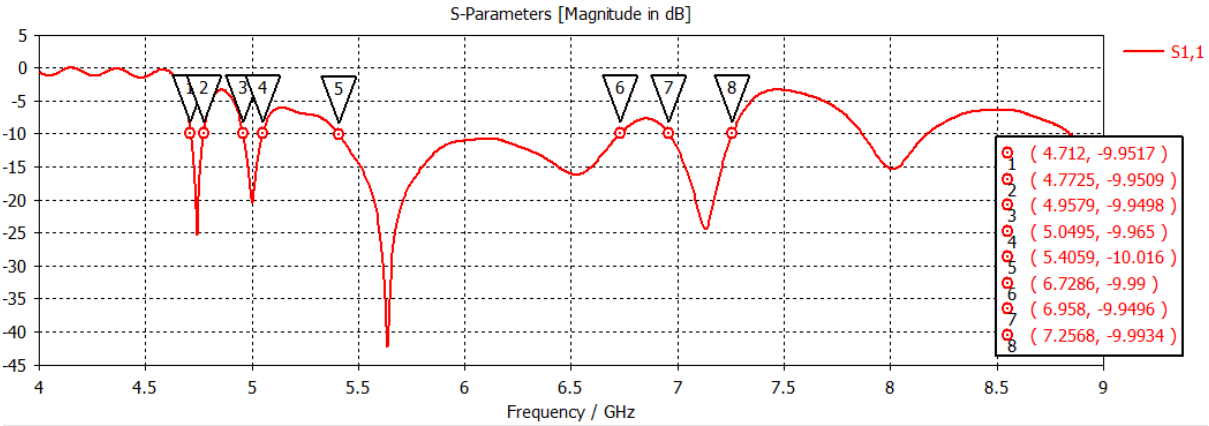

Figure 4.10 S_{11} plot of presented antenna

Here, antenna ground was optimised as a partial ground to achieve the desired results in terms of enhanced bandwidth. Figure 4.11 shows the combined plot of antennas with S_{11} plot against frequency with and without partial ground. The variation in bandwidth at the three bands can be easily identified, and it can be concluded that a partial ground leads to a better performance of the stacked patch antenna. Therefore in the final design, a partially reduced ground is preferred.

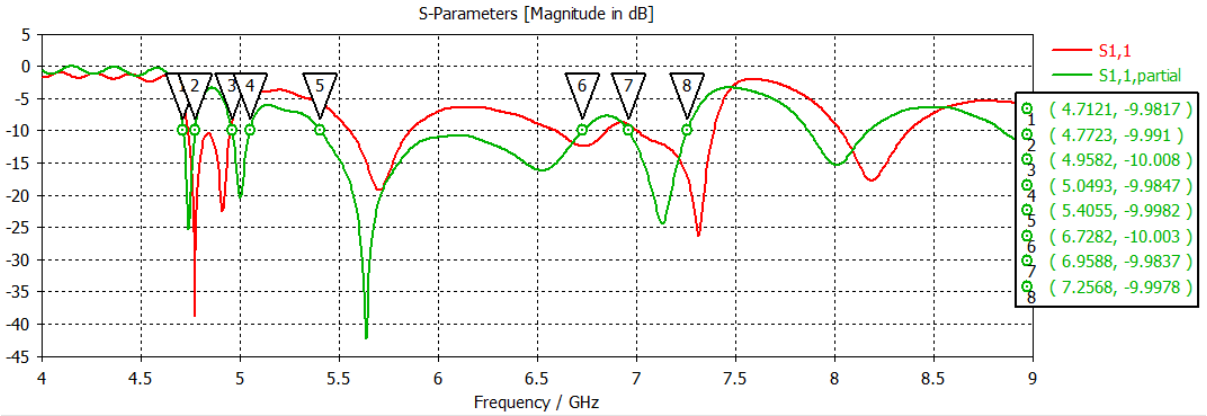

Figure 4.11 Combined plot of antennas S_{11} with and without partial ground

4.2.2.2 Broadband Gain:

The overall broadband gain of the stacked diamond sierpinski gasket is shown in Figure 4.12 that shows a peak gain of 6.833 dBi at 5.5 GHz and average gain of 6 dBi for the entire band. A good gain antenna can be used for long range wireless applications.

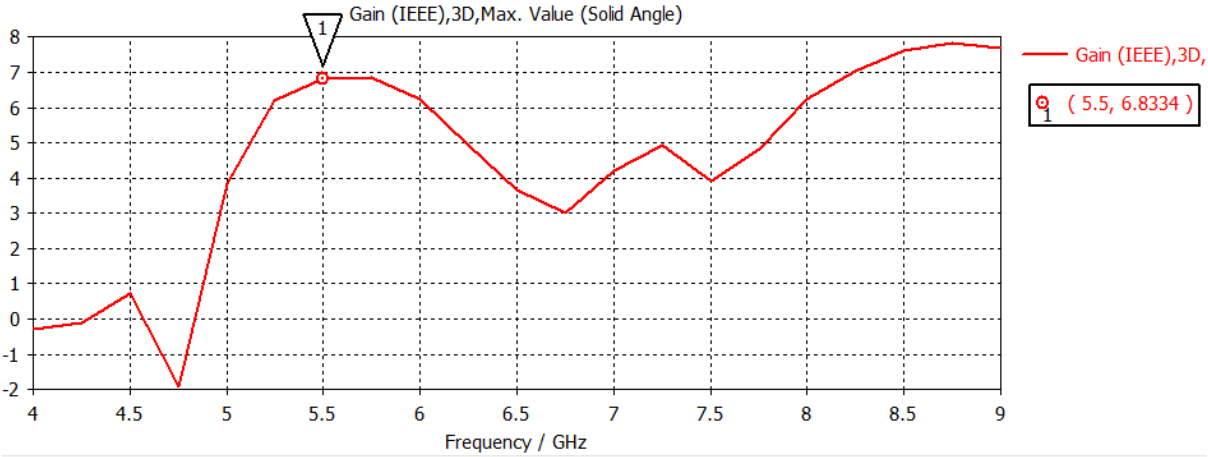

Figure 4.12 Overall broadband gain of the proposed antenna

4.2.2.3 Radiation Pattern:

Figure 4.13 (a) illustrates radiation pattern of antenna in terms of gain at a resonant frequency of 6.5 GHz. The antenna shows a peak gain of 3.316 dBi, and the polar plots of the radiation

pattern are shown in Figure 4.13 (b). The antenna has a major lobe along 171 degrees and a half power beamwidth of 72.2 degrees.

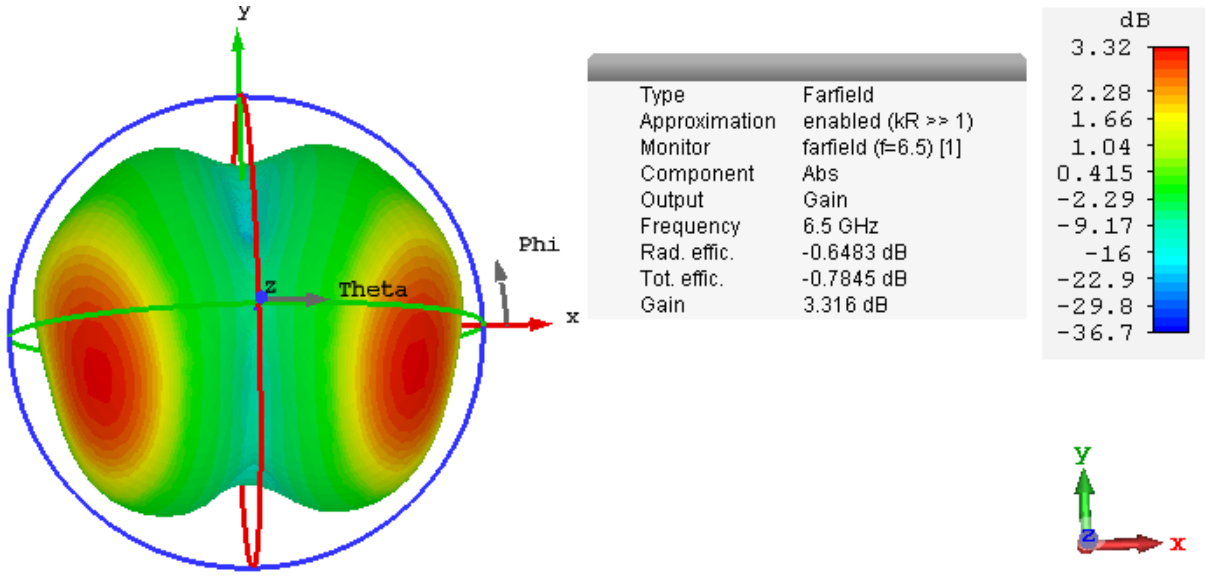

(a)

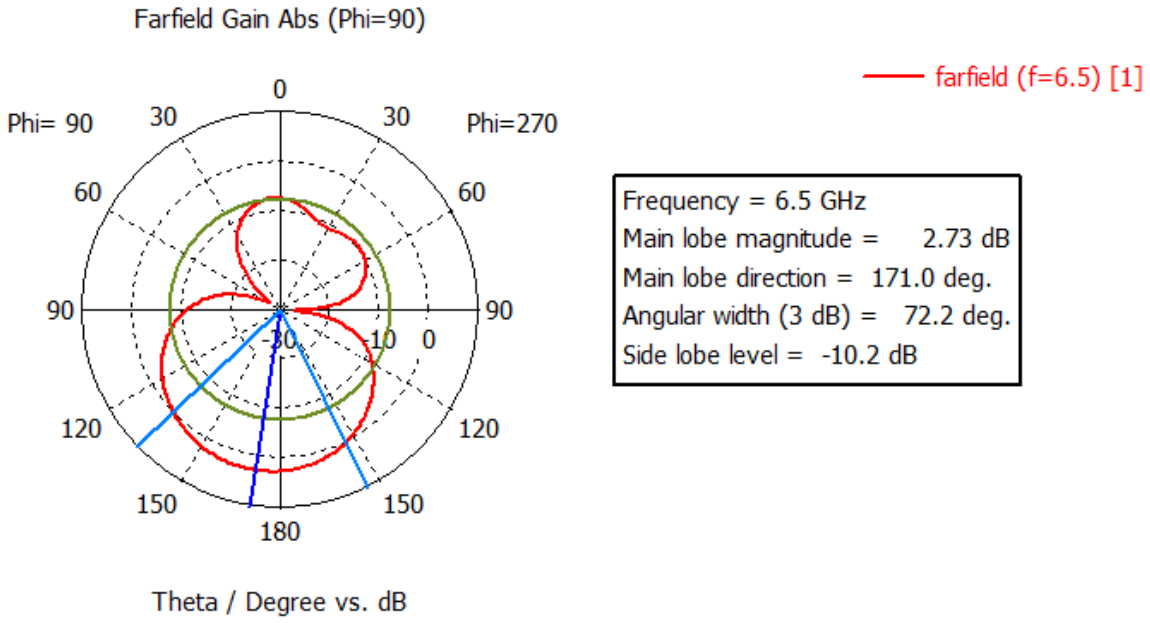

(b)

Figure 4.13 (a) Radiation pattern of presented antenna at 6.5 GHz,
(b) Polar plot of antenna at 6.5 GHz

4.2.2.4 Surface Current Distribution

Figure 4.14(a-d) show current distribution on various layers of antenna for resonant frequencies of 6.5 GHz and 6.15 GHz, when antenna is energized using an aperture coupled feeding in the software. A comparative study of surface current on various layers of antenna leads to the conclusion that top patch is responsible for exciting 6.5 GHz frequency.

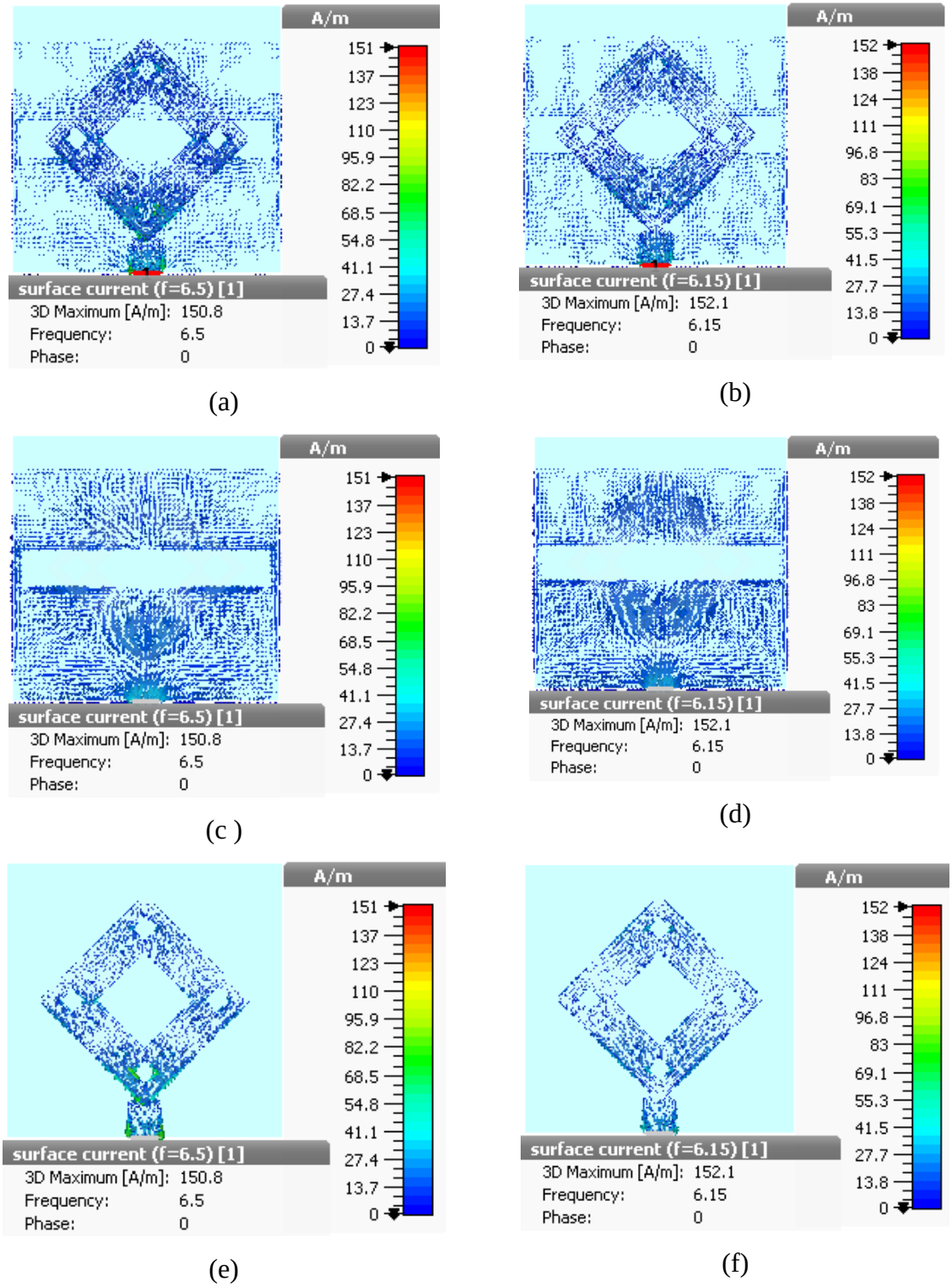

Figure 4.14 Surface current distribution of presented antenna at resonating frequencies (a, c, e) 6.5 GHz (b, d, f) 6.15 GHz

Table 4.3 shows the comparitive analysis of unstacked and stacked diamond fractal geometries in terms of resonant frequencies, impedance BW.

From the comparison analysis of all the two unstacked and stacked diamond shaped sierpinski gasket fractal geometries, the best one among two is geometry 2 i.e., stacked structure. This geometry shows more resonances of good bandwidth as compared to geometry 1. Geometry 2 is covering ultra-wide band and have more applications compared to other one. So, the best geometry among the three is geometry 2.

Table 4.3 Comparison of unstacked and stacked geometries mentioned above

Geometries	**Resonances**	**Impedance BW**	**Gain**	**Applications**
Geometry 1	5.45 GHz, 6.22 GHz, 7.81 GHz	90 MHz, 370 MHz, 390 MHz	7.33 dBi	G band, F band, C band.
Geometry 2	4.74 GHz, 5.00 GHz, 5.63 GHz, 7.13 GHz.	90 GHz, 1.32 GHz, 300 MHz.	6.83 dBi	WLAN, satellite communication, wifi devices, cordless telephone.

4.3 CONCLUSION:

The stacked diamond sierpinski fractal antenna is designed as well as simulated with three level of iteration. Here, active and parasitic patch together are responsible for the multiple resonances generated by the antenna. The partial ground helps in achieving a good bandwidth, and the four resonances are observed at 4.74 GHz, 5.00 GHz, 5.63 GHz, and 7.13 GHz with a bandwidth of 90 MHz, 1.32 GHz and 300 MHz. The antenna possesses a peak gain of 6.833 dBi, and this allows the proposed antenna to be suitable for WLAN, satellite communication, Wi-Fi devices, cordless telephone, and some weather radar systems.

CHAPTER- 5

FABRICATION AND EXPERIMENTALTESTING OF PROPOSED STACKED ANTENNAS

5.1 INTRODUCTION:

This chapter presents the fabrication and experimental testing of the proposed Stacked sierpinski gasket fractal antennas with driven and parasitic patch of same dimensions as mentioned in chapter-3 and stacked diamond shaped sierpinski gasket fractal antenna with same size of driven and parasitic patch as mentioned in chapter 4. The fabrication as well as testing of antenna is conducted to check the applicably of antenna to the practical wireless scenario. The antenna was fabricated on the FR4 substrate, and photolithography (wet etching) process was used for fabrication of antenna. Here, return loss for both the stacked antennas was measured by utilising Agilent's vector network analyzer (VNA) model no E5063A, whose operating frequency range is from 1 to 20 GHz.

5.2 TESTING OF FRACTAL ANTENNAS:

Figure 5.1 depict Agilent's vector network analyzer (VNA) model no E5063A for testing the antenna, whose operating frequency range is from 1 to 20 GHz.

Figure 5.1 Vector network analyzer for testing

5.3 FABRICATION OF STACKED SIERPINSKI GASKET FRACTAL ANTENNAS WITH DRIVEN AND PARASITIC PATCHES OF SAME DIMENSION:

Figures 5.2(a,b,c) depict the top perspective of different layers of fabricated antenna. Figure 5.2(a) shows the top view of stacked sierpinski gasket bow-tie antenna, and Figure 5.2(b) shows the partial ground and the driven patch of bow-tie sierpinski gasket antenna using same

dimensions of active and parasitic patches. Figure 5.2 (c) illustrates the top perspective of strip line as well as of active patch of antenna.

Figure 5.2(a) Stacked bow-tie antenna side view

(b) (c)

Figure 5.2 Photograph of fabricated antenna (b) partial ground and top perspective of fabricated antenna, (c) strip line and the active patch of the fabricated antenna

The antennas were fabricated using the photolithography process, and the flowchart of fabrication process is mentioned in Figure 5.3.

Figure 5.3 Flow chart for the fabrication procedure of the presented antenna

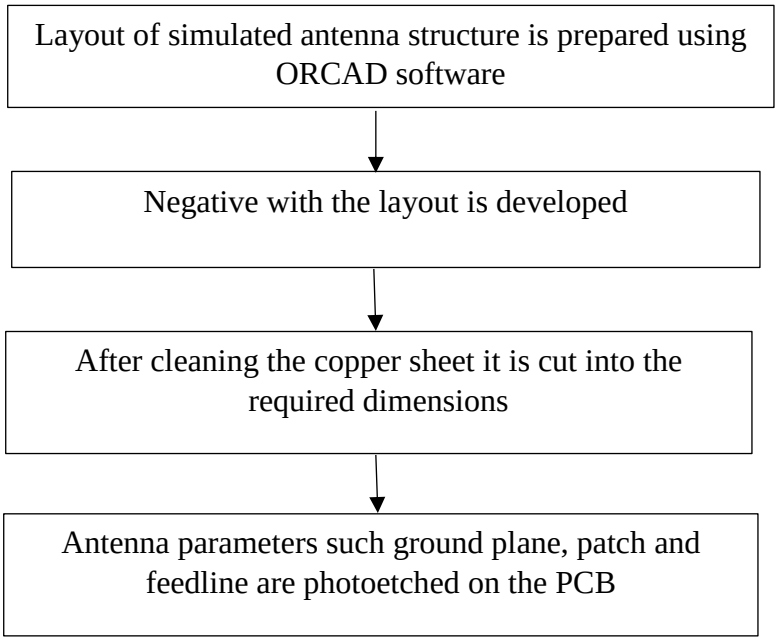

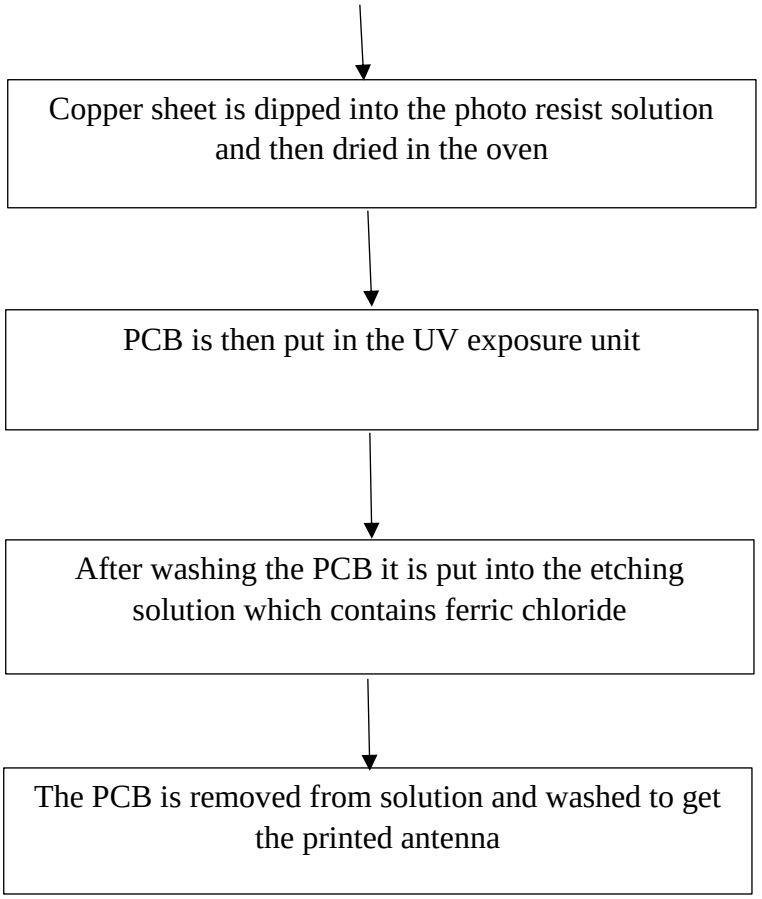

Figure 5.4(a) shows the snap shot of measured results on the VNA and Figure 5.4(b) demonstrates comparative results of simulated and measured S_{11} parameter of the antenna with respect to frequency. The measured results match closely to the simulated ones. A comparison Table 5.1 mentions the details of variation between simulated and measured S parameter values. The main reason for this drift in the frequencies may be attributed to the fabrication errors as well as to impedance mismatch occurring in practical cases.

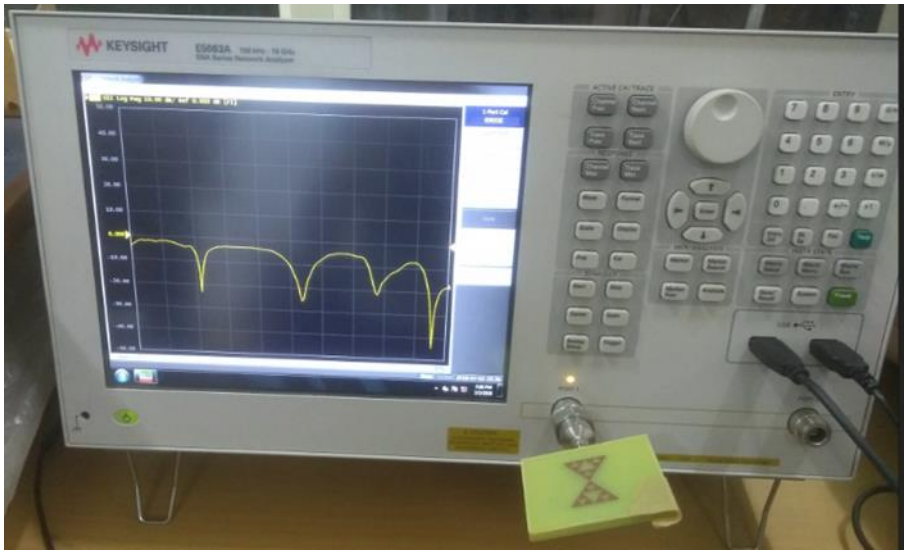

Figure 5.4(a) Measured results on the VNA

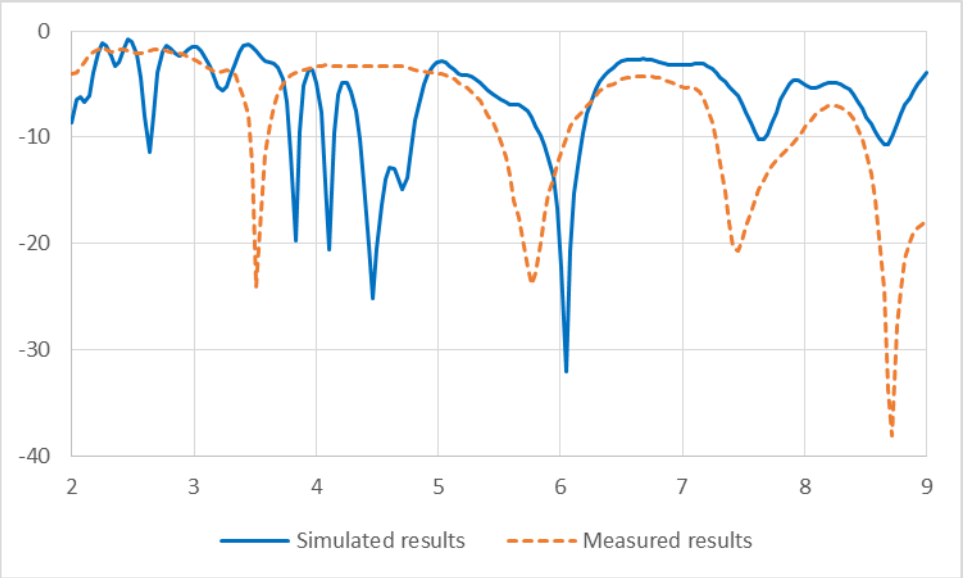

Figure 5.4(b) Comparison of simulated and measured outcomes of presented antenna

Table 5.1 Comparison of results of fabricated antenna

Parameters	**Simulated results**	**Measured results**
Resonant frequency	3.82 GHz, 4.1 GHz, 4.45 GHz, 6.03 GHz	3.512 GHz, 5.763 GHz, 7.452 GHz
Impedance bandwidth	80 MHz, 90 MHz, 440 MHz, 330 MHz	140 MHz, 530 MHz, 670 MHz
Applications covered	Short range Wi-Fi, wireless broadband, some cordless telephone, G band, E band wireless applications.	Short range Wi-Fi, wireless broadband, some cordless telephone, G band, E band wireless applications.

5.4 FABRICATION OF DIAMOND SHAPED STACKED SIERPINSKI GASKET FRACTAL ANTENNA:

Figure 5.4(a, b, c) demonstrates top view of various layers of fabricated antenna. Figure 5.4(a) depicts top view of stacked sierpinski gasket diamond shaped antenna. Figure 5.4(b) indicates the partial ground of the antenna, and Figure 5.4(c) illustrates the top view of parasitic patch. Here, antennas are fabricated using the same photolithography process, as mentioned in flowchart in Figure 5.3.

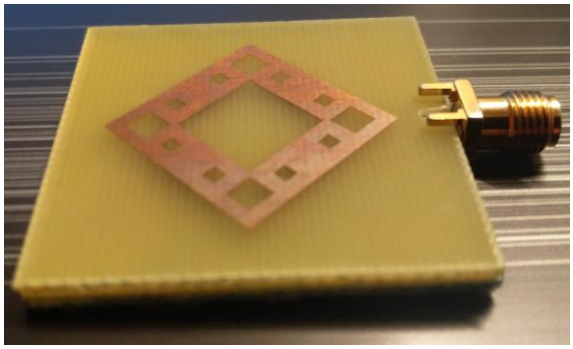

(a)

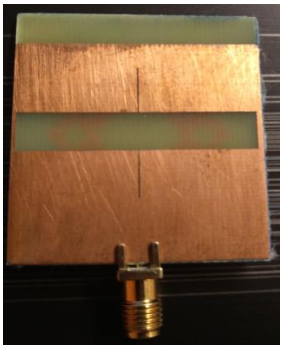

(b) (c)

Figure 5.5(a) Stacked with both layers, (b) Active and ground (c) Parasitic and feed line

The fabricated antenna was tested using a VNA model no. E5063A, and Figure 5.6(a) shows the snapshot of the measured results on the VNA. Figure 5.6(b) indicates comparison of simulated as well as measured outcomes. The results match, but a small variation that is seen in terms of reduction of the impedance bandwidth is because of the mismatch in impedance of the fabricated antenna due to fabrication errors.

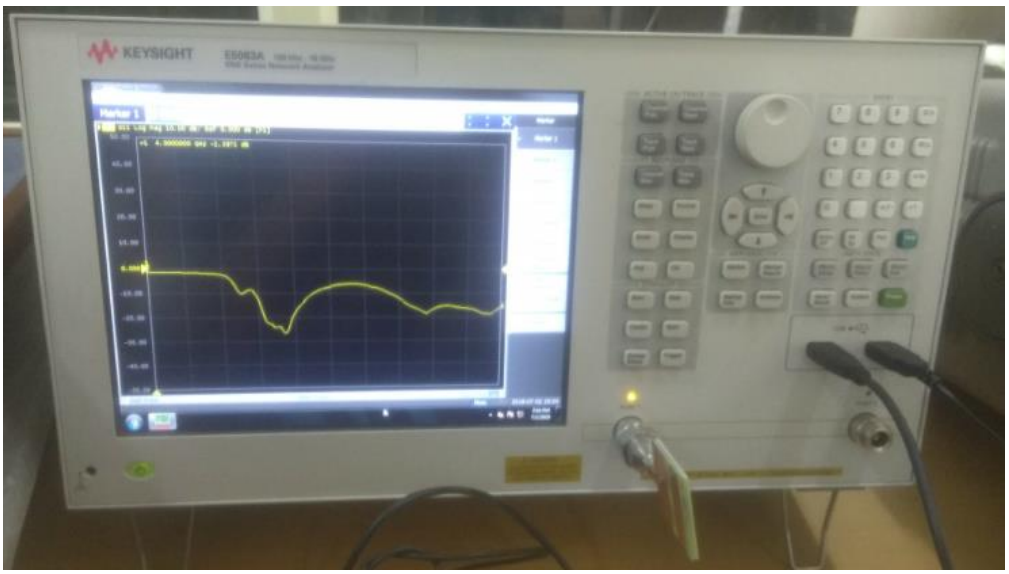

Figure 5.6(a) Measured results on the VNA

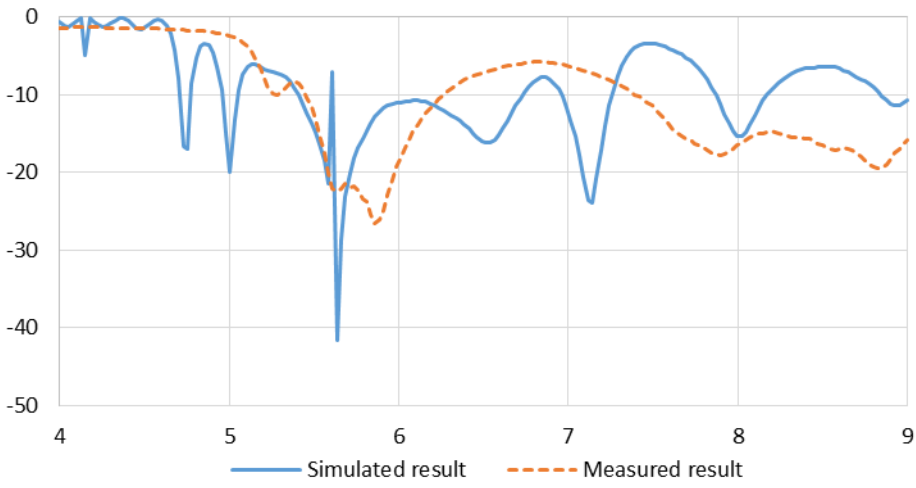

Figure 5.6(b) Comparison of simulated and measured outcomes of presented antenna

Table 5.2 Comparison of results of fabricated antenna

Parameters	**Simulated results**	**Measured results**
Resonant frequency	4.74 GHz, 5.00 GHz, 5.63 GHz, 7.13 GHz	5.88 GHz, 7.91 GHz
Impedance bandwidth	90 MHz, 1.32 GHz, 300 MHz	810 MHz
Applications covered	WLAN,satellite communication, Wi-Fi devices, cordless telephone	WLAN,satellite communication, Wi-Fi devices, cordless telephone

5.5 CONCLUSION:

This chapter presents the fabrication and experimental testing of two stacked antennas that were designed and simulated in chapter-3 and chapter-4. This is seen that simulated as well as measured outcomes approximately match allowing the antenna to be practically suitable for cordless phones, Wi-Fi, satellite communication, military systems and radar communication applications.

CHAPTER- 6

CONCLUSION AND FUTURE SCOPE

6.1 CONCLUDING REMARKS:

The research work presented in this thesis report starts with the study of fractal aperture coupled antennas and stacked antennas with aperture coupled feeding mechanism. A fractal bow-tie antenna is then designed with an aperture coupled feed, and all its radiation properties are studied. Then stacking of this bow-tie antenna with bow-tie patches on a substrate of same FR4 material as the lower one is done. The stacked structure are of three types namely: of the same size, parasitic patch of $3/4^{th}$ size as that of the standard driven patch and driven patch $3/4^{th}$ size as that of standard parasitic patch. On comparing the performance of the three structures, it was observed that stacked structure with same size of driven and parasitic patch had best results, and is therefore preferred for future research also. Based upon this, the next design that has been worked upon is a stacked diamond shaped sierpinski gasket fractal with same size of driven and parasitic patch.

In general, the research work carried out in each chapter is concluded below:

- First geometry is unstacked sierpinski gasket fractal antenna; the proposed antenna operates in the frequency band from 4.04-4.49 GHz and 8.16-8.38 GHz with bandwidth of 380 MHz and 270 MHz, which makes the antenna suitable for the UWB operation (5.3-9.28 GHz), Radio Astronomy Band (5.01-5.03 GHz), as well as IEEE 802.11a WLAN applications (5.15 to 5.825 GHz).
- Second geometry is stacked sierpinski gasket fractal with driven and paracitic of same dimenssion, the proposed antenna has bandwidth of 80 MHz (3.86-3.78 GHz), 90 MHz (4.14-4.05 GHz), 440 MHz (4.79-4.35 GHz) and 330 MHz (6.17-5.83 GHz), which is used for short range Wi-Fi, wireless broadband and some cordless telephone. Also the antenna is suitable for the G band (3.95-5.85 GHz), E band (3.30-4.90 GHz).
- Third geometry is stacked with driven patch smaller than active patch, the proposed antenna has bandwidth of 160 MHz (4.43-4.5 GHz), 1120 MHz (4.80-5.92 GHz), and 420 MHz (7.71-8.13 GHz), which is used for short range Wi-Fi, wireless broadband and some cordless telephone. Also the antenna is suitable for the G band(3.95-5.85 GHz), F band (4.90-7.05 GHz) and C band (5.85-8.20 GHz).

- Fourth geometry is a stacked MSA with active patch smaller than the driven patch, the proposed antenna has bandwidth of 190 MHz (5.15-5.34 GHz) and 1250 MHz (7.10-8.35 GHz), which is used for short range Wi-Fi, wireless broadband and some cordless telephone applications. Also the antenna is suitable for the G band(3.95-5.85 GHz), F band (4.90-7.05 GHz) , C band (5.85-8.20 GHz) and H band (7.05-10.10 GHz).

Chapter four presents two antenna geometry structures and their simulation results.

- First geometry is unstacked diamond shaped sierpinski fractal, the proposed antenna has bandwidth of 90 MHz (5.42-5.51 GHz), 370MHz (6.04-6.41 GHz), and 390 MHz (8.00-7.61GHz), which is used for some weather radar system, short range Wi-Fi, wireless broadband and cordless telephone. Also the antenna is suitable for the G band (3.95-5.85 GHz), F band (4.90-7.05 GHz) and C band (5.85-8.20 GHz) wireless applications.
- Second geometry is stacked diamond sierpinski fractal antenna, developed as well as simulated with three level of iterations. Here, active and parasitic patch together are responsible for the multiple resonances generated by the antenna. The partial ground helps in achieving a good bandwidth the four resonance at 4.74 GHz, 5.00 GHz, 5.63 GHz, and 7.13 GHz with a bandwidth of 90 MHz, 1.32 GHz and 300 MHz. The antenna possesses a peak gain of 6.833 dBi, and this allows presented antenna to be adequate for WLAN, satellite transmission, Wi-Fi devices, cordless telephone, and some weather radar systems.

Table 6.1 indicates comparison of all simulated as well as measured outcomes of presented antenna in terms of resonant frequency, return loss, impedance BW as well as gain of antenna.

Table 6.1 Comparison between simulated and measured results

Geometry	**Simulated**			**Measured**		
	Simulated Resonant Frequency (GHz)	**Simulated Impedance Bandwidth (MHz)**	**Simulated Gain (dB)**	**Measured Resonant Frequency (GHz)**	**Measured Impedance Bandwidth (MHz)**	**Measured Gain (dB)**
Stacked bow-tie shaped structure	3.82, 4.1, 4.45, 6.03	80, 90, 440, 330	5.40	3.512, 5.763, 7.452	140, 530, 670	-
Stacked diamond shaped structure	4.74, 5.00, 5.63, 7.13	90, 1320, 300	6.83	5.88, 7.91	810	-

6.2 FUTURE SCOPE:

As the zone of fractal antenna engineering research is still in its early stages, there are numerous potential outcomes for future work on this topic. Number of fractal geometries exist that have desirable antenna characteristic. Thus, other type of fractal structures can be studied for future work that can be applicable in various antenna applications. A new pattern of fractal can be developed for antenna arrays. Fractal antennas can be studied in various areas, such as in expanding wireless market. The polarizations of these antennas need to be studied for such applications. Fractal antennas with different geometries for circular and elliptical polarization can be researched upon in future.

Meta-materials can also be used to design antennas; a meta-material is referred to metallic or semiconductor material with its properties dependent on inner-atomic structure instead of on atomic composition themselves. Visible light rays can be bend by certain metamaterials, and such behaviour can also be noticed at infrared wavelengths.

The work on MPA design using aperture coupling can be extended to:

• Using stacked MPAs, by utilising different values of dielectric constant and different material of substrate.

• Embedding different slot shapes on patch and ground.

• Use of impedance matching network for enhancement of the impedance bandwidth.

Antenna can be designed with varying substrates for different stacked layers. These can be used to achieve multiband and broadband properties for multiple wireless applications. Antennas can be designed for microwave imaging applications for detecting malignant cells in the human body as well.

REFERECES

[1] T. Rappaport, *Wireless Communication: Principles and Practise*, 2nd edition, Pearson, 1996.

[2] A. Goldsmith, *Wireless Communication*, Cambridge University Press, 2005.

[3] K. Siakavara and N. Nasimuddin, *Microstrip Antennas*, Chapter-9, In Tech., 2011.

[4] B. Mandelbrot, *The Fractal Geometry of Nature*, San Francisco, CA: Freeman, 1983.

[5] D. H. Werner and S. Ganguly, "An overview of fractal antenna engineering research," *IEEE Antennas Propag. Mag.*, vol. 45, no. 1, pp. 38-57, 2003.

[6] Z. U. Islam, M. Rahman, N. Muhammad, Z. Ahmed, F. K. Lodhi, and M. Haneef, "Dual band second order modified sierpinski monopole reduced size fractal antenna," in *Proc. IEEE ICET*, Islamabad, Pakistan, 2016, pp. 18-19.

[7] S. Neha, P. C. Dalsamia, and H. J. Kathiriya, "Analysis of koch snowlflake fractal antenna for multiband application," *Int. J. Engg. Res. Technol*., vol. 3, no. 4, pp. 2150-2152, 2014.

[8] N. S. Dandgavhal, M. B. Kadu, and R. P. Labade, "Design of microstrip patch antenna with koch snowflake geometry for multiband application," in *Proc. IEEE IBSS*, Mumbai, India, 2015, pp. 6578-6584.

[9] M. T. Islam and M. Samsuzzamanb," A compact patch antenna for ultrawideband application," in *Proc. IEEE ICISET*, Dhaka, Bangladesh, 2016, pp. 1-4.

[10] L. C. Ping, C. K. Chakrabarty, and R. A. Khan," Design of Ultra-Wideband Slotted Microstrip Patch Antenna," in *Proc. IEEE MICC*, Malaysia, 2009, pp. 41–45.

[11] A. Gorai, M. Pal, and R. Ghatak, "A compact fractal-shaped antenna for ultrawideband and bluetooth wireless system with wlan rejection functionality," *IEEE Antennas Wireless Propag. Lett.*, vol. 16, pp. 2163-2166, 2017.

[12] E. E. M. Khaled, A. A. R. Saad, and D. A. Salem, "A Proximity-Fed Ultra-Wideband Annular Slot Antenna with Band-Notch Characteristics Via a Split- Ring Parasitic Element," in *Proc. IEEE EUCAP*, Prague, 2012, pp. 1-5.

[13] A. S. W. Ghattas and E. E. M. Khaled," A proximity-fed ultra-wide band patch antenna with four frequency-band notches," in *Proc. IEEE JEC-ECC*, Egypt, 2013, pp. 125-129.

[14] K. Ruchandani and M. Kumar," A novel CPW fed octagonal aperture UWB antenna with 5 GHz/6 GHz band rejection by h shaped slot," in *Proc. IEEE IC4*, Indore, India, 2015, pp. 14.

[15] A. S. W. Ghattas and E. E. M. Khaled, "A compact proximity-fed ultra-wide band patch antenna with four notched-band characteristics design and implementation," in *Proc. IEEE CSNDSP*, Manchester, UK, 2014, pp. 612-616.

[16] R. A. Abdulhasan, R. Alias, A. A. Awaleh, and A. O. Mumin." Design of circular patch microstrip ultra-wideband antenna with two notch filters," in *Proc. IEEE I4CT*, Kuching, Malaysia, 2015, pp. 464-467.

[17] S.Sarkar and S.S.Prasad, "A compact proximity-coupled bow-tie microstrip antenna using stubs for ultra-wideband application," in *Proc. IEEE ICIEV*, Dhaka, Bangladesh, 2013, pp. 1-5.

[18] A. Agarwal and A. Kaur, "A dual band stacked aperture coupled antenna array for WLAN application," *Microw. Opt. Technol. Lett.*, vol. 59, vol. 3, pp. 648– 654, 2016.

[19] J. Y. Sze, C. G. Hsu, and J. Y. Shiu, "Small CPW-fed band-notched ultra-wideband rectangular aperture antenna," *IEEE Antennas Wireless Propag. Lett.*, vol. 7, pp. 513 - 516, 2008.

[20] M. Khan, D. Ketharnath, V. K. Dandu, and D. Chatterjee, "UWB L-probe proximity fed V-slot patch antenna for early detection of breast cancer," in *Proc. IEEE ASP*, Vancouver, Canada, 2015, pp. 1882-1883.

[21] C. Elavarasi, and T. Shanmuganantham, "CSRR loaded sierpinski gasket fractal antenna for multiband applications," in *Proc. IEEE ICETT*, Kollam, India, 2016.

[22] S. D. Targonski and D. M. Pozar, "Design of wideband circularly polarized aperture-coupled microstrip antennas," *IEEE Trans. Antennas Propag.*, vol. 41, no. 2, pp. 214-220, 1993.

[23] Q. Rao, T. A. Denidni, and R. H. Johnston, "A new aperture coupled microstrip slot antenna," *IEEE Trans. Antennas Propag.*, vol. 53, no. 9, pp. 2818-2826, 2005.

[24] C.A Balanis, *Antenna Theory: Analysis and Design*, 2nd edition, United States of America, John Wiley & Sons Inc., 1997.

[25] V. P. Patil, "Enhancement of bandwidth of rectangular patch antenna using two square slots techniques," *Int. J. Engg. Technol.*, vol. 3, no. 2, pp. 1-12, 2012.

[26] J. P. Gianvittorio and Y. Rahmat, "Fractal antennas: A novel antenna miniaturization technique and applications," *IEEE Antenna Propag. Mag.*, vol. 44, no. 1, pp. 20-36, 2002.

[27] A. Kaur, "Semi spiral G-shaped dual wideband microstrip antenna with aperture feeding for WLAN /WiMAX/U-NII band applications," *Int. J. Microw. Wireless Technol.*, vol. 8, no. 6, pp. 931-941, 2016.

[28] A. Kaur and G. Singh, "A review paper on fractal antenna engineering," *Int. J. Advance Res. Elect. Electron. Instrum. Engg.*, vol. 3, no. 6, pp. 2320-3765, 2014

[29] A. Kaur, R. Khanna, and M. V. Kartikeyan, "A stacked sierpinski gasket fractal antenna with a defected ground structure for UWB/WLAN/radio astronomy/Stm link applications," *Microw. Opt. Technol. Lett.*, vol. 57, no. 12, pp. 2786-2792, 2015.

[30] N. Cohen, "Fractal antenna applications in wireless telecommunications," in *Proc. IEEE EIF, New England*, 1997, pp. 43-49.

[31] A. Azari, "A new super wideband fractal microstrip antenna," *IEEE Trans. Antennas Propag.*, vol. 59, no. 5, pp. 1724-1727, 2011.

[32] A. Bisht and M. Gupta, "A cup-shaped slotted microstrip patch antenna for UWB applications," in *Proc. IEEE ICACCA*, Dehradun, India, 2016, pp. 1-4.

[33] D. D. Krishna., M. Gopikrishna, C. K. Anandan, P. Mohanan, and K. Vasudevan, "CPW-fed koch fractal slot antenna for WLAN/WiMAX applications," *IEEE Trans. Antennas Propag. Lett.*, vol. 7, pp. 389-392, 2008.

[34] A. Aggarwal and M. V. Kartikeyan, "Pythagorean tree: A fractal patch antenna for multi-frequency and ultra-wide bandwidth operations," *Progress Electromagn. Res.*, vol. 16, pp. 25-35, 2010.

[35] P. Tang, "Scaling property of the koch fractal dipole," *IEEE Int. Symp. Antennas Propag. Dig.*, vol. 3, pp. 150-153, 2000.

[36] N. S. Jibhkate and P. L. Zade, “A compact multiband plus shaped CPW fed fractal antenna for wireless applications,” in *Proc. IEEE GET*, Coimbatore, India, 2016, pp. 1-5.

[37] S. Jagdeesha, R. M. Vani, P. V. Hunagund, and P. Hegde, “Two element self-similar plus fractal antenna for wireless applications,” in *Proc. IEEE CRT*, Ujire, India, 2013,pp. 1-5.

[38] S. Jagadeesha, R. M. Vani, and P. V. Hunugund, “Stacked plus shape fractal antenna for wireless application,” *Int. J. Electron. Commun. Engg. Technol.*, vol. 3, no. 1, pp. 286-292, 2012.

[39] I. Singh and V. S. Tripathi, “Micro-strip patch antenna and its applications: A survey,” *Int. J. Comput. Technol. Appl.*, vol. 2, vol. 5, pp. 1595-1599, 2011.

[40] M. Singh, A. Basu, and S. K. Koul, “Design of aperture coupled fed microstrip patch antenna for wireless communication,” in *Proc. IEEE IC*, New Delhi, India, 2006, pp. 1-5.

[41] S. Yadav, R. Choudhary, U. Soni, B. Peswani, and M. M. Sharma, “ Koch curve fractal antenna for Wi-MAX and C Band wireless applications,” in *Proc. IEEE ICCIT*, Noida, India, 2014, pp. 490-494.

[42] K. J. Vinoy, K. A. Jose, V. K. Varadan, and V. V. Varadan, “Resonant frequency of hilbert curve fractal antennas,” *IEEE Antennas Propag. Int. Symp.*, vol. 3, pp. 648-651, 2001.

[43] C. Puente, J. Romeu , R Pous , X. Garcia, and F. Benitez, “Fractal multiband antenna based on sierpinski gasket,” *IEEE Electron. Lett.*, vol. 32, pp. 1-2, 1996.

[44] R. K. Mishra, R. Ghatak, and D. R. Poddar, “Design formula for sierpinski gasket pre fractal planar-monopole antennas,” *IEEE Antennas Propag. Mag.*, vol. 50, no. 3, pp. 104-107, 2008.

[45] R. Kieda and M. Kitlinski, “Sierpinski monopole antenna uniplanar feeding technique,” in *Proc. IEEE ICMRWC*, Poland, 2004, pp. 477-480.

[46] S. E. El-Khamy, M. A. Aboul-Dahab, and M. Elkashlan, “A simplified koch multiband fractal array using windowing and quantization techniques*,”* in *Proc. IEEE USNC*, USA, 2000, pp. 1716-1719.

[47] D. M. Pozar and S. M. Duffy, “A dual-band circularly polarized aperture- coupled stacked microstrip antenna for global positioning satellite,” *IEEE Trans. Antenna Propag.*, vol. 45, no. 11, pp. 1618-1625, 1997.

[48] D. H. Werner, “An Overview of fractal electrodynamics research,” in *Proc. IEEE ACE*, California, 1995, pp. 964-969.

[49] K. J. Vinoy, K. A. Jose, V. K. Varadan, and V. V. Varadan, “Resonant frequency of hilbert curve fractal antennas,” in *Proc. IEEE USNC*, Boston, 2011, pp. 648-651.

[50] R. G. Hohlfeld and N. Cohen, “Self-similarity and the geometric requirements for frequency independence in antenna, fractals,” *IEEE Trans. Antennas Propag.*, vol. 7, no. 1, pp. 79-84, 1999.

[51] C. P. Baliarda, J. Romeu, and A. Cardama A., “The koch monopole: a small fractal antenna,” *IEEE Trans. Antennas Propag.*, vol. 11, pp. 1773- 1781, 2000.

[52] A. Sundaram, M. Maddela, and R. Ramadoss, “Koch-fractal folded-slot antenna characteristics,” *IEEE Antenna Wireless Propag. Lett.*, vol. 6, pp. 219-222, 2017.

LIST OF PUBLICATIONS

Communicated to

- K. Laxmi *et al.,* "Comparative analysis of unstacked and stacked bow-tie antenna structures for wireless applications," in *Proc*. *ICIECE*, Hyderabad, India, 2018.
- K. Laxmi *et al*., "Design and development of a stacked diamond shaped sierpinski gasket antenna with a defected ground structure for WLAN applications," *Int. J. Bentham Sci.*, 2018.